ACADEMY OF SCIENCES OF RUSSIAN FEDERATION
INSTITUTE FOR DYNAMICS OF THE GEOSPHERES

REGIONAL ANALYSIS of FORMER SOVIET UNION PEACEFUL NUCLEAR EXPLOSIONS RECORDED in the FORMER SOVIET UNION

V.A. Laushkin, S.I. Oreshin, V.M. Ovtchinnikov

(Sponsored by **EOARD**, special contract **SPC-94-4065**)

Principal investigator

V.V. Adushkin

"11" November, 1995

Moscow, 1995

REPORT DOCUMENTATION PAGE

Form Approved OMB No. 0704-0188

1. AGENCY USE ONLY (Leave blank)	2. REPORT DATE	3. REPORT TYPE AND DATES COVERED
	11 November 1995	Final Report

4. TITLE AND SUBTITLE

Regional Analysis of Former Soviet Union Peaceful Nuclear Explosions Recorded in the Former Soviet Union

5. FUNDING NUMBERS

F6170894W0750

6. AUTHOR(S)

Dr. V Adushkin

7. PERFORMING ORGANIZATION NAME(S) AND ADDRESS(ES)

Russian Academy of Sciences
18 Lenininsky Prospekt
Moscow 11797
Russia

8. PERFORMING ORGANIZATION REPORT NUMBER

N/A

9. SPONSORING/MONITORING AGENCY NAME(S) AND ADDRESS(ES)

EOARD
PSC 802 BOX 14
FPO 09499-0200

10. SPONSORING/MONITORING AGENCY REPORT NUMBER

SPC 94-4065

11. SUPPLEMENTARY NOTES

12a. DISTRIBUTION/AVAILABILITY STATEMENT

Approved for public release; distribution is unlimited.

12b. DISTRIBUTION CODE

A

13. ABSTRACT (Maximum 200 words)

This report results from a contract tasking Russian Academy of Sciences as follows: The contractor will investigate, collect, digitize and analyze a sample of regional Soviet peaceful nuclear explosions to define signal characteristics.

14. SUBJECT TERMS

EOARD

15. NUMBER OF PAGES

53

16. PRICE CODE

N/A

17. SECURITY CLASSIFICATION OF REPORT	18. SECURITY CLASSIFICATION OF THIS PAGE	19. SECURITY CLASSIFICATION OF ABSTRACT	20. LIMITATION OF ABSTRACT
UNCLASSIFIED	UNCLASSIFIED	UNCLASSIFIED	UL

CONTENTS

Introduction

Until the late 80's information on Soviet underground nuclear explosions, let alone seismic recording on Soviet soil, were not generally available to the seismological community. The dramatic changes since then have resulted in access to a wide variety of seismic data from Soviet explosions. In this report we present a data set, unique to the field of seismic verification. The data includes a large number of waveforms from in-country seismological station Borovoye for the Soviet peaceful nuclear explosions with announced yields and origin times, some with physical and mechanical conditions at the test site. The waveforms were recorded by digital station of different types. In this report we have summarized and rewiewed information on 122 explosions, and 55 waveforms in this data set, which contains recordings obtained in the course of more than 15 years. As the characteristics of recording instruments were changing during this period of time available information on instrument calibrations is also described and reviewed.

We also have attempted to describe the observed pecularities of P-wave by using a simple source function and magnitude correction which take in attention such parameters as the velocity of longitudinal wave, density, moisture, gase content and depth of explosion. More detail analysis was conducted for the explosions conducted in salt as there is representative sample and they were observed on local distances.

Peaceful nuclear explosions

122 explosions were conducted in USSR in the period from 1965 to 1988. The map in Figure 1 shows the location of explosions sites, which are squares and seismological station Borovoye which is asterisk. The size of square scaled by magnitude of explosion. The boundaryes of major tectonic elements of the USSR are portrayed with lines in Figure 1 showing that the parts traverse a diversity of tectonic structures.

Information on date, origin time, location and body wave magnitude m., reported by ISC, is compiled in Table 1. Precise times, based on nonseismological information, have been collected for 78 explosions (Nuclear Explosions in the USSR, 1994) . The epicenter estimates, entered in Table 1, are limited to those of ISC as they are the only type determination consistently applied all the explosions, with exception for 15 explosions which location based on nonseismological information (marked by *) have published by Sultanov et all (1993). To estimate the errors in locations and origin times , obtained at ISC, we have compared nonseismological and seismological information. We have recieved the systematic bias about 2.6±0.4 sec which agrees with the estimation of the arrival time curve of P-wave by (Kogan S.D.,1976). The root mean square error in location has been estimated as 6±4 km. As results the origin times for 44 explosions , based on seismological data , are the ISC origin times corrected for the systematic bias.

Table 2 summurizes the information on the type of environmental media contained explosions and summerizes the quantitive value such parameters of media as the longitudinal wave,ν , density,ρ, gaseous content,γ ,and moisture,ω. The information on yield,q, and reduced depth

is also compiled in Table 2. The velocity , entered in Table 2 , was estimated by seismic and acustic sounding. The density was estimated from the sample of rock. The relative moisture is the part of water which was vaporized from the sample of rock , heated up to 100^0 C. The relative gaseous content is the number of gases which was recieved from the sample of rock , heated up to 1000^0 C. In that cases when the environmental media was unhomogenity we used the parameter as the average for the layer which thick is equal two caverne radius r_c. That is

$$\alpha = \sum_i \frac{\alpha_i}{2r_c} h_i \qquad \text{and} \qquad \sum_i h_i = 2r_c \qquad \text{where}$$

a_i , h_i are the value parameter of i in the layer with the thick of h_i. The table shows that the parameters are limited $1.8 \le v \le 4.4$ km/sec, $170 \le h \le 2500$ m, $1.7 \le \rho \le 3.0$ g/cm^3, $0 \le \omega \le 30\%$, $0 \le \gamma \le 40\%$, $300 \le \Delta \le 3300$ km.
Of all the explosions with known conditions at the test site until we have collected:

53 records with P-wave,

25 records with Lg wave,

7 records with surface wave.

Plot record section of vertical component for some explosions is shown on the Figure 2. The analysis of these records shows that from the distances about 1960 km the maximum amplitude in the S- and Lg- waves becomes much lower than the P-wave amplitude. In the range of epicentral distances from 300 km to 1600 km the maximum amplitude of S- and Lg-waves is a comparable with P-wave amplitude. The exception is the set of explosions in the Uralsk region, being carryed out in salt, at the distance about 1160 km. The amplitudes of S- and Lg-waves were lower than for P-wave ones in about 3-4 times. It is worth mentioning that nonseismological information on the yield or the conditions at the test site of explosion, carryed out on

24/09/83 (origin time is 05h09m57.4 sec), shown in Table 1 are not seems to be correct. In the same conditions of media where this set was carryed and similarity of waveform of all six explosions, the maximum amplitude of P-wave differs a great deal from the amplitude for other explosions. The magnitude, derived from the data of in-country stations , for the explosion under question is 4.85 while for other 5 explosions is in the range 5.18-5.19. It follows the the yield is 3.9 kt according to formula (12) below. The relative yield estimation on Borovoye data , presented in (Sultanov D.J. et all,1993) is 3.4. That is the yield is about 2.5 kt.

The Borovoye Geophysical Observatory

The Borovoye Geophysical Observatory is one of the oldest seismic stations of the world in terms of the digital seismic recording. The observatory has the richest archive, comprizing the digital material of various kinds of recording systems working from 1965 until nowadays. There is therefore the Borovoye station draw the attention of the world community of scientists.

Station characteristics

The Borovoye seismic station (BRVK) with coordinates $53^0.083$ North, $70^0.250$ East is located in the North Kazakstan about 70 km to the South from Kokchetav town.

In terms of geology the Borovoye region presents as a flat denudation country and hills with altitude change from 160 to 500 meters. The region is made up of Paleozoic and prior-Paleozoic dislocated rocks, breaked by intrusive igneous rocks of various age. On the surface there are loose stuff, presented by loosened granite, sands, loamy soils, clays the thick of which may vary from severel meters to several hundreds meters. The P-wave velocity in the layers varies from 0.65 to 2.8 km/sec. From seismic studies it follows that the thick of granite layer is estimated as 8 - 10 km and basalt layer - as 35 km. The thick of crust vary from 40 to 50 km.

The main tectonic element in the block structure of the tectonic framework of the region is extremely complicated by the faults of the first order, they having north-west direction. The faults of the second order have different directions. From gravity and magnetic studies it

follows that the faults of the first order penetrate through the granite layer as a whole.

At the station place the granite layer comes out on the surface and almost monolithic granite are on the deep to vary from 6 to 10 meters.

The tectonic structure of the North Kazakhstan is known from the deep seismic studies which was carried out by means of numerous profiles (Antonenko A.,N.,1984). The main profile was the profile of extent about 1000 km from Temirtau to Petrorpavlovsk (Figure 3).

Side by side with deep faults the massifes of rocks of Agnostozoic era are the main tectonic element of North Kazakhstan structure. The Borovoye station is situated on one of these massifes, named Kokchetav anticlinorium. Note should be taken that the crust was studied in detail in the profile zones. The profile observation system of seismic waves have given the possibility to record the waves refracted on Moho and on the discontinuties in the crust. Thus the refracted waves from Moho discontinuty were well observed along the profiles on large distances. However, beneath the region of Borovoye the sharp eliminate of amplitudes of P-waves refracted on Moho discontinuty was being observed. Dissapearance of the waves refracted on Moho may be explained by existance of strongly dislocated zones in the mantle beneath Borovoye region.

The second main rezult, carried out by means of deep seismic study was that beneath Borovoye region the crust discontinuties were not revealed. So the crust under the place may be considered as "transparent".

Until 1972 the seismometers of the station were installed in the gallery in weekly cracked granite with absolute altitude of about 340 meters and from 1972 they were installed in the mine with deep of 15 meters from the surface and altitude to be equal 315 meters in practically monolithe granite.

The seismic station was set up for the observation of seismic waves generated by nuclear explosions at the Nevada test site. The first records of seismic waves in Borovoye showed that the signals from Nevada were two or three times greater than would be expected.

While developing of seismic recording several kinds of system of registration were used. The first digital system, known as KOD, began recording in 1966 and continuous worked from 1967 to 1973 (AdushkinV.,V.,and V.,A. An, 1992). It was based on three component short-period seismometers and was one of the oldest digital system, operating in the world in 1960s and 1970s. Later, other digital systems were installed. They are known as STR-SS and STR-TSG. The digital system STR-SS was intended mainly for low-gain recording and the system STR-TSG, which operated with twenty four channels, most recorded a two gain levels. STR-TSG system is based on long-period and short period Kirnos seismometers. Both STR-SS and STR-TSG have been operating from 1973 up to the present. The dynamic range of every channel makes up 60 dB. The Figure 4 demonstrates amplitude-frequency response of some digital channels, operating at Borovoye station.

The seismic station is situated at the place of low level of noise to be both natural and industrial. The amplitude of the noise of short period range vary from one to ten nanometers and the noise of long period range composes 100-200 nm.

MORFOLOGY of SEISMIC SIGNALS

General description

When P-waves propagate through the Earth the high frequencies are preferetially attenuated so that individual pulse are smeared out and may overlap. Also, as the recording system has limited pass band, signals are further distorted on recording. Analysis and interpretation of short-period seismograms may thus be difficult. The regional observed waveform is very complicate due to the path of propagation. There are a number of seismic phases (reflected, refracted, converted), generated on the stucture inhomogenities in the crust and upper mantle. This is a good aid to interpreting short-period explosion recordings is to compute seismograms using model of the Earth, source and seismograph and try and match these the observed.

Comparing waveform of P-wave from PNE at the distances 300-3300 km reveals their substantial discrepency. Nevetheless, it takes place an extremal similarity that could be presented as a similar initial part of P-waves, which is consisted of three phases that are clear. At the distances up to 1000 km the first arrival has a period of 0.5-0.6 sec, the period of the second phase is 1.0-1.2 sec, then again the phase with period about 0.5-0.6 sec appears. It is that the maximum amplitude is associated. At the distances about 1700 km another picture can be observed: the first arrival has a larger period, the second has a smaller one and the third phase has a larger period again. The example of record is shown on the Figure 4. This pecularity is typical for events on the regional distances.

At the distances up to 1000 km the first arrivals is a wave with the velocity about 8.15 km/sec associated with Moho discontinuity. At the far

distances the first arrival seems a head wave propagating in the upper mantle with the velocity about 8.48 km/sec and associated with discontinuity on the depth about 150-200 km.

However, there is the substantial pecularity of records of the events carried out to the North of the station. The maximum amplitude in P-wave is at the later time than for the signals arriving from other directions. The maximum amplitude arrival time, **Pmtime**, and the first arrival time, **Ptime**, summerizes in the Table 3 and the examples of seismogram shown on the Figure 6 (a,b,c). It can see that the time delay of the maximum amplitude arrival relative the first time arrival is about 40 sec (Figure 6 a,b). The parameters of explosions , shown on the Figure 6, presented in Table 4. One can assume, that observed pecularity could be related with the disturbance of Moho discontinuity to the North from Borovoye station, which was detected by deep seismic sounding, or with a vast fault which, as supposed, penetrates to the upper mantle (Antonenko,1972).

Incident angle and azimuth

Because of strong interference in the wave-train in the 5 sec interval after the first arrival , which contains, possibly, two arrivals on the distance of 1200 km and three arrivals on the distance 1700 km, detailed study was carryed out of these arrivals.

First of all the incident angle and azimuth of coming waves were estimated by using the analysis of eigenvalue and eigenvector of the covariance matrix in the moving time window. For instantanous motion u_i (i=1,2,3), the cross power matrix is

$$C_{kl} = \frac{1}{N}\sum_{t=1}^{N} u_{tk}u_{tl} \quad \text{k,l=1,2,3} \qquad (1)$$

The eigenvalue λ and eigenvector ν of matrix C can be found from

$$(C - \lambda^2 I)v_k = 0, \quad \text{m=1,2,3} \qquad (2)$$

and are ordered by size, I is the unit matrix. The normalized eigenvalue $\nu=(\nu_{1m}, \nu_{2m}, \nu_{3m})$ corresponding to the largest eigenvalue λ may than be used as an estimate of the dominant signal direction. The apperent azimuth and angle of incidence are to be found from

$$\tan Az = \frac{v_{1e}}{v_{1n}}, \qquad Cost = v_{1z}. \qquad (3)$$

The size of λ can be used as a measure of the stability of this procedure since it will be a unit for purely rectilinear motion. These directional parameters are calculated from the particle motion of the code, hence they do not necessarily give the actual direction of propagation. The polarization parameters as rectilinearity was also calculated. The measures of rectilinearity are based on the eigenvalue of covariance matrix employed in the power technique:

$$rect = 1 - (\lambda_3 + \lambda_2) / 2\lambda_1, \qquad (4)$$

where $\lambda_1, \lambda_2, \lambda_3$ are the eigenvalues (largest to smallest) of cross power matrix C. In Figure 7 we display the wave field measured introduced above. For the P-waves, the estimated azimuth is close to the source-receiver azimuth of 274° for the explosions on the distance about 1160 km and is close to the source-receiver azimuth of 255° for the explosions on the distance of 1715 km. The azimuth is stable for the interval of about 6 sec relatively the first arrival. The azimuth , incident angle and the ratio of middle λ_2 and maximun eigenvalue λ_1 related to different phase arrival are presented in Tables 5,6. One can see from Tables 5,6 that there are common features in behavious of measure of wavefield parameters. The apparent azimuth is fairly stable for the first 6 sec of the seismogram, but some fluctuations are seen

and the systematic azimuth deviation with increasing time too. Effect of decreasing azimuth with time is observed. The apparent angle of incidence shows considerable variability but clearly indicates on the distance of 1716 km on the increasing in the begining of signal and the decreasing in the end of signal. The maximun value is 44.5° . On the distance of 1160 km the incidence angle decreases with time.

High rectiliniarity values are generally associated with stable azimuth values, and at the places where the azimuth fluctuates, the values indicate the waves are not rectilinear. We have done this analysis in order to try to define the wave types which can appear on the seismogram.

Summarizing the results of above analysis it is possible to conclude that there are several linear-polarized signals in the first arrival of P-wave with different velocities. It is usual for the distance of 1716 km. We can suggest that these pecularities are related to the reflected and refracted waves in the upper mantle . In particular the first arrival on the distance up to 1000 kilometers is the head wave Pn due to Moho discontinuty, and the following phase due to more deep part of the upper mantle. On the distance up to 1000 kilometers the Pn phase marked the arrival of longitudinal waves traveling in the uppermost mantle. It is known from numerous investigations that the travel time curve of Pn is practically a straight line. The slope has been found about 13.5 sec/degree, which corresponds to wave velocity about 8.2 km/sec (Passechnik , 1972) . The first arrival on the distance 1716 km do not mark as P wave refracted in gradient velocity of the earth because of the complex waveform. We suppose that the first arrival can be a head wave generated by the discontinuity on the depth 150-200 km. It can be supposed that there is low velocity layer on this depth because the great amplitude on the 2-3 sec after the first arrival. The maximum amplitude arrival seems to be reflected wave from discontinuty on the depth of 150-200 km.

On the distance above 2100 km the waveform is very simple and we can suppose that the P-wave is the first arrival because of the longer period and faster velocity.

Source model and scaling low

In the vibrating sphere problem, an explosion is modelled at and beyond some critical distance - elastic radius, where the material behaves elastically by a radial stress applied uniformaly over a spherical surface . The spherical surface which separates inelastic from elastic response has been called by equivalent cavity by Sharpe (1942).

For a step in pressure $p(t)=P_0H(t)$,where P_0 is the amplitude of the pressure applied to the inside of a spherical surface at $r=R_0$ and H(t) is Heaviside step function that is $H(t)=1$ for $t\geq 0$ and $H(t)=0$ for $t<0$.

In this case

$$u_p(r,\omega)=\frac{P_0}{4}\frac{R_0^3}{\mu}\left[\frac{v_p}{v_p^2-\left(\frac{v_p}{2v_s}\right)^2 R^2\omega^2+\iota\omega v_p R_0}\right]\frac{e^{-\iota k_p r}}{r}, \qquad (5)$$

where v_p and v_s are longitudinal and shear velocity , μ is shear modulus, and ω and k_p are angular frequency and wavenumber , respectively.

Spectra of the direct P-wave have the obvious asymtotic behaviour

$$u_p(r,\omega)=\frac{P_0}{4}\frac{R_0^3}{v_p\mu}\frac{e^{-\iota k_p r}}{r} \quad \text{for } \omega<\omega_0 \qquad (6) \quad \text{and}$$

$$u_p(r,\omega)=\frac{P_0}{4}\frac{R_0^3}{v_p\mu}\left(\frac{2v_s}{R_0\omega}\right)^2\frac{e^{-\iota k_p r}}{r} \quad \text{for } \omega>\omega_0 . \qquad (7)$$

With the base on these relations one can get the corner frequency ω_0 as a point of crossing of the asymtotes that is the point where high-frequency asymptote crosses low-frequency one.

To use these relations for the explosions conducted in the media with different mechanical and physical behaviour we need the knowledge what way $P_0 R_0^3$ depends on above parameters. The work (Laushkin V.A. and Ovtchinnikov V.M., 1992) offers a simple model for taking into account a physical and mechanical features of media when estimating the yield of explosion. It was done by introducing the magnitude correction according to the following relation

$$\Delta m = 1.56\left(1.75\log\frac{\nu}{\nu_0} + 0.39\log\frac{\rho}{\rho_0} + 3\log(1+2.9\omega) + 3\log(1+0.62\gamma) + \Delta m_h\right) \quad (8)$$

$$\Delta m_h = 0.32\log\frac{h}{\bar{h}} \text{ for } h/\bar{h} \le 5 \quad (9)$$

and $$\Delta m_h = 0.32\log\frac{h}{\bar{h}} + 0.4 \text{ for } h/\bar{h} \le 5, \quad (10)$$

where $\bar{h} = 100\sqrt[3]{q}$.

In this relation ν is the longitudinal velocity, ρ is density of media contained explosion , ω is relative moisture , γ is relative gase content, h is a depth of and q is yield of explosion. Index 0 refers to some reference media for which the relation between m and q is known. Figure 8 presents the relation m=f(q) for the explosions from Table 1 and magnitude correcton from Table 2. On this picture (a) we can see a substantial scatter of experimental data relatively the line

$$m=0.77\log q + 4.4. \quad (11)$$

Introducing the magnitude correction , calculated in according to above relation , we can see from picture (b) that the experimental points place more close relatively the line

$$m-\Delta m=0.81\log q+4.4. \qquad (12)$$

The relative root mean square error is 20%.

To give a physical interpretation of magnitude correction Δm we will use the Sharpe model as the the source function.

Following Nersesov et all (1991) let the changing of elastic energy of media be proportional to the yield of explosion, e.g. $\Delta U=Cq$, where C depends upon the characteristics of media , containing the explosion. On the other hand, the work made on the elastic radius by pressure P_0 is

$$\Delta U = \Delta W = \int_{R_0}^{R_0+\Delta R} 4r^2 P_0 \pi dr = 4P_0 R_0^3 \left(\frac{\Delta R}{R_0}\right)\pi , \qquad (13)$$

where ΔR is motion of elastic boundary due to pressure P_0 on R_0. From the condition that the pressure on R_0 is equal to the elastic limit of media ,Y we can write

$$Y = k_s\left(\frac{\Delta R}{R_0}\right), \qquad (14)$$

where k_s is adiabatic volumetric modulus.

Therefore , from relations (13), (14) we receive

$$P_0 R_0^3 = K_c q \quad , \qquad (15)$$

where $K_c = \frac{Ck_s}{4Y\pi}$ is constant of nonlinear coupling of. explosion, which depends on the elastic parameters of media , porosity, moisture and gase content.

For the spectral amplitude for the regional (teleseismic) distances by using the Sharpe model as the spectral source function we can write

$$U(\Delta,\omega)=\frac{K_c}{K_e}qG(\Delta)\exp\left(\iota\pi ft^*\right)\left|1-\left(\frac{\omega}{\omega_0}\right)^2+i\frac{2\omega}{\omega_0}\right|^{-1}, \qquad (16)$$

where K_e is constant of elastic coupling, $G(\Delta)$ is the geometrics spreading function, and t^* is the apparent attenuation.

Body wave magnitude for the period of 1 sec is

$m=\log|u|+b(\Delta)$.

To take in attention the low-frequency asymptote it follows

$$m=\log q+\log\left(\frac{K_c}{K_e}\right)+b(\Delta)., \qquad (17)$$

where $b(\Delta)$ is the calibrate function (Vanek U, Kondorskaiy N.,V., et all, 1962) that is the correction for the attenuation on the path of propagation and the geometrics spreading.

Thus magnitude correction, introduced above, $\Delta m=\log\left(\frac{K_c}{K_e}\right)$.

Spectra of some explosions in salt

The instrument -corrected amplitude spectra can be parametrized as

$$U(\omega,\Delta)=S(\omega)G(\Delta)\exp(\frac{-\pi ft}{Q}) \qquad (18)$$

where $S(\omega)$ is the source spectrum, $G(\Delta)$ is the geometric spreading function and last term is the apparent attenuation for the travel time t. The geometric spreading of head wave is a complicated function of the velocity gradient in mantle and it is probably frequency-dependent. Therefore, a simple parametrization such as (18) is not likely to be applicable to a head wave for a broad frequency band and distances range. To exclude the influence a geometric spreading function we have compared four explosions conducted in salt in close distance range.

Spectra were calculated for two time windows which duration was 2 sec. The begining time of windows relatively the first arrival time were 0 sec and 3 sec consequently.

P-wave spectra of four explosions with yield 103, 58, 23, and 9.3 kt in salt , corrected for instrument responce and for attenuation (Q-factor is equal 1200) are shown in Figures 9,10. We assumed that the corner frequency of these explosions should be below 4 Hz, and the low-frequency asymptote is proportional ω^{-1} for the signal spectra of head wave (Zvolinskiy,1958) and is the plate for the signal spectra for the second time windows. The high-frequency asymptote is proportional $\omega^{-\eta}$ where $\eta=3$ for ahead wave and $\eta=2$ for the second time window.

We can see from Figure 9 that the spectra for the first time window were very slightly modulated by periodic function. In the low frequency range the specta fall down as ω^{-1} . Spectra of the second time window on Figure 10 have distinct relative minimum, and is the plate in the low-frequency range. Figures 9 and 10 show also the theoretical far-field amplitude spectra of the Sharpe model calculated for explosion with yield of 100 kt following Evernden et all (1986). The corrected spectra of as the first time window as the second time window doesn't show a clear corner frequency, perhaps, because of the complicated multiple arrival. However it should be emphasized that the low-frequency asymptote is in the agreement with our assumptions. But we can not explain observed relative minimun in spectra, as usual, by influence of the depth of events.

Conclusion

1. There was collected seismological and nonseismological information on 122 peaceful underground nuclear explosions on the territory of the USSR which includes the data on date, origin time, coordinates, depth, yield, magnitude as well as data on parameters of media, where the explosions were carried out, such as velocity of the longitudinal waves, density, moisture, gaseous content.

2. 53 digital short-period records of Borovoye seismic station situated in the North Kazakhstan were collected, edited, and analysed. The channel responces accompany these records.

3. The analysis of prominent pecularities of waveforms allows to assume that on the distances up to 1000 km first arrival is a head wave generated by Moho, and on the distances in the range 1200 -1900 km first arrival is a head wave associates with the discontinuity in upper mantle at the depth about 150-200 km.

4. The influence of media features on the seismic efficiency was investigated, and the relation between the characteristics of media parameters of explosion on the base of Sharpe model was established.

5. The explosions carryed out to the North from the seismic station have a specific waveform due to, probably, the disturbance of Moho discontinuity.

6. The spectra of explosions in salt, corrected for instrument responce and for attenuation, don't show a clear corner frequency , perhaps because of the complicated multiple arrival.

REFERENCES

Adushkin V.V., and V.A. An, Seismic and monitoring of underground nuclear explosions at Borovoye Geophysical Observatory, *Izv. Acad. Sci. USSR, Phys.Solid Earth,* #12, 1990 (in Russian).

Antonenko A.,N., Deep Structure of the Crust in Kazakhstan, *Nauka, Alma-Ata,* 1984 (in Russian).

Denny M.,D., The explosion Seismic Source Function:Models and Scaling Law Reviewed, *Explosion Source Phenomenology,Geophys. Monograph,65,*1991.

Evernden,J.F., C.B. Archambeau, and E. Cranswick, An evaluation of seismic decoupling and underground nuclear test monitoring using high-frequency seismic data, *Rev. of Geophys.,24* , 143-215,1986.

Kogan S.D., An experimental travel-time curve for P wave and lateral inhomogenity of the mantle, *Dokl. Acad. Nauk USSR* ,230, 1318-1321 (in Russin).

Kogan S.Y., Methods of Seismic Energy Estimation,*Nauka, p.151,*1975.

Laushkin V.A., and V.M. Ovtchinnikov , Yield Estimation under known condition at the test site, EOS, 1992.

Nersesov I.L., et all, The USSR-USA works on the seismic monitoring of nuclear explosions, *Nauka,*1991 (in Russian).

Nuclear Explosions in the USSR, Peaceful Underground Nuclear Explosions, *Helping information,* #4 ,1994 (in Russian)

Pasechnik I.P., The Characterisrics of Seismic Waves generated by Nuclear Explosions and Earthquakes, *Nauka,* 1970 (in Russian)

Sharpe, J.A., The production of Elastic Waves by Explosion Pressures. I. Theory and Empirical Field Observations , *Geophys., 7*,144,1942.

Sultanov D.J. et all, Investigation of seismic efficiency of Soviet peacefulnuclear explosions conducted in various geological condition. *report,Part 1, IDG* , 1993

Zvolinskiy N.,V., Reflected and Head Waves on the Boundary of Two Half-space. II, *Izv. Acad. Sci. USSR, Geoph.*,#1,1958 (in Russian).

Tables

Table 1

Date	Media	Lat,N	Long E	GMT,hhmmss	Depth,m	Yield	m
15.01.65	sandstone	49.93500	79.00936	60000.800	178.0	140.00	6.3
30.03.65	limestone	53.00000	55.80000	80000.000	1360.0	4.60	
10.06.65	limestone	53.00000	55.80000	70000.000	1350.0	7.60	
14.10.65	aleurolite	49.99064	77.63572	40000.200	4.8	1.10	
22.04.66	salt	47.90000	47.70000	25803.600	160.0	1.10	4.7
30.09.66	clay	38.80000	64.50000	55952.800	1532.0	30.00	5.1
6.10.67	clay	57.71000	65.22000	70002.500	172.0	0.30	4.7
21.05.68	salt	38.89000	68.10000	35910.000	2400.0	47.00	5.4
1.07.68	salt	47.85000	47.72000	40200.900	600.0	27.00	5.5
21.10.68	aleurolite	49.72786	78.48628	35200.000	30.0	0.24	
12.11.68	aleurolite	49.71244	78.46133	73000.000	32.0	0.72	
2.09.69	limestone	57.35000	54.77000	45957.400	1208.0	7.60	4.8
8.09.69	limestone	57.31000	55.03000	45956.400	1212.0	7.60	4.9
26.09.69	argillaceons sandstone	45.88000	42.49000	65955.900	712.0	10.00	5.6
6.12.69	limestone	43.79000	54.75000	70257.500	407.0	31.00	5.8
25.06.70	salt	52.20000	55.00000	45954.000	700.0	2.30	4.9
12.12.70	limestone	43.87000	54.78000	70057.400	497.0	84.00	6.1
23.12.70	limestone	43.81000	54.82000	70057.300	740.0	75.00	6.0
23.03.71	limestone	61.39000	56.22000	65956.400	128.0	45.00	5.5

Table 1

Date	Media	Lat,N	Long E	GMT,hhmmss	Depth,m	Yield	m
2.07.71	argillite,sandstone	67.66000	62.00000	170001.075	542.0	2.30	4.7
10.07.71	glay	64.20000	54.77000	170001.335	465.0	2.30	5.2
19.09.71	dolomite	57.76000	41.40000	110001.075	610.0	2.30	4.5
4.10.71	limestone	61.61000	47.22000	100000.104	595.0	2.30	4.6
22.10.71	salt	51.61000	54.45000	50000.700	1142.0	15.00	5.2
22.12.71	salt	47.87000	48.22000	65956.300	986.0	64.00	6.0
11.04.72	clay	37.36000	62.07000	60002.000	1720.0	14.00	4.9
9.07.72	salt	49.78000	35.40000	70002.000	2480.0	3.80	4.8
20.08.72	clay	49.40000	48.06000	30000.005	490.0	6.60	5.7
4.09.72	apatite ore	67.73000	33.10000	70006.000	130.0	2.10	4.6
21.09.72	sandstone,clay	52.19000	51.94000	90000.312	490.0	2.30	5.0
3.10.72	clay	46.86000	44.87000	90000.175	490.0	6.60	5.0
24.11.72	dolomite,glay	52.14000	51.80000	90000.043	678.0	2.30	4.5
24.11.72	limestone,sandstone	51.85000	64.18000	100000.230	425.0	6.60	5.2
15.08.73	clay	42.70000	67.41000	20000.018	600.0	6.30	5.3
28.08.73	sandstone	50.58000	68.40000	30000.035	400.0	6.30	5.2
19.09.73	aleurolite	45.68000	67.80000	30000.177	615.0	6.30	5.1
30.09.73	salt	51.66000	54.54000	50000.348	1144.0	10.00	5.2
26.10.73	limestone	53.63000	55.38000	60000.000	2026.0	10.00	4.8

Table 1

Date	Media	Lat,N	Long E	GMT,hhmmss	Depth,m	Yield	m
8.07.74	limestone	53.68000	55.10000	60000.000	2120.0	10.00	4.6
14.08.74	argillite	68.94000	75.83000	150000.188	534.0	7.60	5.4
29.08.74	argillite,sandstone	67.23000	62.10000	150000.394	583.0	7.60	5.0
2.10.74	limestone	66.10000	112.65000	10000.000	100.0	1.70	4.6
7.12.74	argillite	49.92000	77.65000	55956.900	75.0	1.70	4.7
25.04.75	salt	48.10000	47.20000	50003.000	583.0	0.35	
12.08.75	sandstone,aleurolite	70.76000	126.93000	150000.590	500.0	7.60	5.2
29.09.75	salt	69.60000	90.47000	110000.428	834.0	7.60	4.8
29.03.76	salt	49.60000	45.00000	70029.000	990.0	10.00	5.0
29.07.76	salt	47.81000	48.10000	45958.000	1000.0	58.00	5.9
5.11.76	dolomite	61.52000	112.73000	35959.983	1525.0	15.00	5.3
26.07.77	salt	69.54000	90.51000	170000.218	850.0	13.00	5.0
10.08.77	granit	50.95580	110.98330	220000.099	500.0	8.50	5.0
20.08.77	tuff	64.13000	99.60000	220000.775	600.0	8.50	5.0
10.09.77	argillite	57.29000	106.23000	160000.184	550.0	7.00	4.8
30.09.77	salt	47.85000	48.13000	65955.900	1500.0	9.30	5.0
14.10.77	salt	47.85000	47.72000	70000.000	582.0	0.10	
30.10.77	salt	47.85000	47.72000		582.0	0.01	
9.08.78	sandstone,aleurolite	63.65000	125.34000	180000.790	570.0	22.00	5.6

Table 1

Date	Media	Lat,N	Long E	GMT,hhmmss	Depth,m	Yield	m
24.08.78	dolomite	65.87000	112.56000	180000.350	575.0	19.00	5.1
12.09.78	salt	47.85000	47.72000	50000.000	584.0	0.08	
21.09.78	sandstone,aleurolite	66.53000	86.26000	150000.190	886.0	16.00	5.2
7.10.78	dolomite	61.53000	112.87000	235957.000	1530.0	13.00	5.2
17.10.78	salt	47.81000	48.09000	45956.600	971.0	73.00	5.8
17.10.78	aleurolite,sandstone	63.21000	63.26000	140000.160	600.0	23.00	5.5
30.11.78	salt	47.85000	47.72000	80000.000	590.0	0.06	
18.12.78	salt	47.78000	48.14000	75956.300	630.0	103.00	5.9
10.01.79	salt	47.85000	47.72000	80000.000	581.0	0.50	
17.01.79	salt	47.96000	48.14000	75955.700	995.0	65.00	6.0
12.08.79	dolomite	61.86000	122.22000	180000.208	982.0	7.60	4.9
6.09.79	conglomerate tuff	64.06000	99.62000	180000.313	599.0	7.60	4.9
16.09.79	sandstone	48.24000	38.12000	90000.000	903.0	0.30	
4.10.79	clay	60.66000	71.44000	160000.026	837.0	21.00	5.4
7.10.79	dolomite	61.85000	113.12000	210000.222	1547.0	15.00	5.0
24.10.79	salt	47.79000	48.11000	55956.700	982.0	33.00	5.8
16.06.80	limestone	53.00000	55.80000	60000.000	1400.0	3.00	
25.06.80	limestone	53.00000	55.80000	60000.000	1300.0	3.00	
8.10.80	salt	46.79000	48.29000	60000.209	1050.0	8.50	5.2

Table 1

Date	Media	Lat,N	Long E	GMT,hhmmss	Depth,m	Yield	m
1.11.80	salt	60.79000	97.57000	130000.419	724.0	8.00	5.2
10.12.80	aleurolite,sandstone	61.68000	67.00000	70000.056	2490.0	15.00	5.3
25.05.81	clay,aleurolite	68.21000	53.50000	50000.320	1510.0	37.60	5.5
2.09.81	dolomite,limestone	60.59000	55.70000	35959.986	2090.0	3.20	4.4
26.09.81	salt	46.82000	48.28000	50000.275	1050.0	8.50	5.2
26.09.81	salt	46.79000	48.27000	50359.941	1050.0	8.50	5.3
22.10.81	dolomite	63.79000	97.54000	135957.500	580.0	8.50	5.1
30.07.82	dolomite	53.81000	104.13200	210002.280	854.0	8.50	
4.09.82	sandstone	69.20000	81.65000	180000.580	960.0	16.00	5.3
25.09.82	gabbro,aleurolite	64.33000	91.80000	180000.184	550.0	8.50	5.2
10.10.82	dolomite,argillite	61.53000	112.87000	50000.221	1510.0	16.00	5.3
16.10.82	salt	46.77000	48.22000	60000.148	1057.0	13.50	5.4
16.10.82	salt	46.77000	48.24000	60500.075	1100.0	8.50	5.2
16.10.82	salt	46.77000	48.22000	61000.102	991.0	8.50	5.2
16.10.82	salt	46.75000	48.20000	61500.169	973.0	8.50	5.2
10.07.83	salt,angidrite	51.36250	53.30610	40000.010	917.0	13.50	5.3
10.07.83	salt,angidrite	51.36670	53.32720	40459.930	917.0	13.50	5.3
10.07.83	salt,angidrite	51.38000	53.33970	40959.870	840.0	13.50	5.3
24.09.83	salt	46.78310	48.31520	50000.030	1050.0	8.50	5.2

Table 1

Date	Media	Lat,N	Long E	GMT,hhmmss	Depth,m	Yield	m
24.09.83	salt	46.78780	48.29720	50500.030	1060.0	8.50	5.1
24.09.83	salt	46.76720	48.31060	51000.075	920.0	0.00	5.0
24.09.83	salt	46.74940	48.30250	51500.144	1100.0	8.50	5.2
24.09.83	salt	46.75390	48.28940	51959.994	950.0	8.50	5.4
24.09.83	salt	46.76580	48.27440	52500.000	1050.0	8.50	5.3
21.07.84	salt	51.39050	53.35140	30459.714	960.0	13.50	5.3
21.07.84	salt	51.37140	53.33690	30959.835	844.0	13.50	5.4
11.08.84	clay,sandstone	65.07000	55.08000	190000.196	759.0	9.50	5.3
25.08.84	clay	61.88000	72.10000	190000.328	726.0	8.50	5.3
27.08.84	apatite ore	67.77000	33.00000	60000.049	175.0	3.60	4.7
28.08.84	limestone	60.82000	57.10000	25959.836	2065.0	3.20	4.4
28.08.84	limestone	60.70000	57.50000	30459.906	2075.0	3.20	4.4
17.09.84	granit	55.83420	87.52610	210000.029	557.0	10.00	5.0
27.10.84	salt	46.90000	48.15000	60000.099	1000.0	3.20	5.0
27.10.84	salt	46.94000	48.12000	60459.998	1000.0	3.20	5.0
18.06.85	argillite,limestone	60.17000	72.50000	40000.106	2850.0	2.50	
18.07.85	sandstone,aleurolite	65.99390	41.03810	211500.289	772.0	8.50	5.1
19.04.87	limestone	60.62000	57.20000	40000.106	2056.0	3.20	4.5
19.04.87	limestone	60.80000	57.50000	40459.981	2015.0	3.20	4.5

Table 1

Date	Media	Lat,N	Long E	GMT,hhmmss	Depth,m	Yield	m
7.07.87	dolomite,argillite	61.50000	112.83000	0.710	1527.0	13.00	5.1
24.07.87	dolomite,argillite	61.46000	112.78000	20000.720	1515.0	13.00	5.1
12.08.87	salt	61.46000	112.79000	13000.710	815.0	3.20	5.0
3.10.87	salt	47.62000	56.20000	151500.032	1000.0	8.50	5.2
22.08.88	glay	66.32000	78.55000	161958.260	830.0	16.00	5.3
6.09.88	angidrite	61.33000	47.96000	161958.680	820.0	7.50	4.8

Table 2

Date	Media	Yield	Hreduced	Mcor	Velocity	Density	Moisture	Gaseous	Dm	m
15.01.65	sandstone	140.00	0.34							6.3
30.03.65	limestone	4.60	8.18							
10.06.65	limestone	7.60	6.87							
14.10.65	aleurolite	1.10	0.46							
22.04.66	salt	1.10	1.55	0.061	4.60	2.20				4.7
30.09.66	clay	30.00	4.93	0.221	1.80	2.00	0.150	0.15	-0.122	5.1
6.10.67	clay	0.30	2.57	0.131	2.10	2.00	0.350	0.12	0.585	4.7
21.05.68	salt	47.00	6.65	0.187	4.18	2.16			-0.071	5.4
1.07.68	salt	27.00	2.00	0.096	4.60	2.20			-0.094	5.5
21.10.68	aleurolite	0.24	0.48							
12.11.68	aleurolite	0.72	0.36							
2.09.69	limestone	7.60	6.14	-0.102	4.30	2.50	0.030	0.20	-0.039	4.8
8.09.69	limestone	7.60	6.16	-0.103	4.30	2.50	0.030	0.20	-0.044	4.9
26.09.69	argillaceons sandstone	10.00	3.30	0.166	2.50	2.20	0.150	0.15	0.207	5.6
6.12.69	limestone	31.00	1.30	-0.264	4.40	2.40	0.100	0.40	0.282	5.8
25.06.70	salt	2.30	4.90	0.218	4.20	2.20			-0.012	4.9
12.12.70	limestone	84.00	1.13	-0.283	4.40	2.40	0.100	0.40	0.252	6.1
23.12.70	limestone	75.00	1.75	-0.222	4.40	2.40	0.100	0.40	0.348	6.0
23.03.71	limestone	45.00	0.36	0.190						5.5

Table 2

Date	Media	Yield	Hreduced	Mcor	Velocity	Density	Moisture	Gaseous	Dm	m
2.07.71	argillite,sandstone	2.30	4.11	0.196	3.80	2.60			-0.121	4.7
10.07.71	glay	2.30	3.52	0.175	2.73	2.44	0.190	0.14	0.481	5.2
19.09.71	dolomite	2.30	4.62	-0.087	5.30	2.48	0.020	0.06	0.008	4.5
4.10.71	limestone	2.30	3.79	-0.115	4.50	2.40	0.030	0.20	-0.024	4.6
22.10.71	salt	15.00	4.63	0.213	4.20	2.20			-0.020	5.2
22.12.71	salt	64.00	2.46	0.125	4.60	2.20			-0.049	6.0
11.04.72	clay	14.00	7.14	0.177	1.80	2.00	0.140	0.14	-0.243	4.9
9.07.72	salt	3.80	15.89	0.066	4.45	2.16			-0.185	4.8
20.08.72	glay	6.60	2.62	0.134	2.10	2.70	0.300	0.12	0.512	5.7
4.09.72	apatite ore	2.10	1.00	0.002						4.6
21.09.72	sandstone,clay	2.30	3.71	0.182	3.50	2.70	0.050	0.08	0.144	5.0
3.10.72	glay	6.60	2.61	0.133	2.10	2.20	0.180	0.12	0.033	5.0
24.11.72	dolomite,glay	2.30	5.14	-0.078	3.80	2.60	0.050	0.24	0.009	4.5
24.11.72	limestone,sandstone	6.60	2.26	0.113	4.10	2.50	0.000	0.15	0.010	5.2
15.08.73	clay	6.30	3.25	0.164	2.25	2.40	0.120	0.15	-0.026	5.3
28.08.73	sandstone	6.30	2.17	0.108	2.80	2.40	0.100	0.12	0.022	5.2
19.09.73	aleurolite	6.30	3.33	0.167	3.20	2.55	0.050	0.12	0.046	5.1
30.09.73	salt	10.00	5.31	0.218	4.20	2.20			-0.012	5.2
26.10.73	limestone	10.00	9.40	-0.161	4.70	2.50	0.020	0.20	-0.095	4.8

Table 2

Date	Media	Yield	Hreduced	Mcor	Velocity	Density	Moisture	Gaseous	Dm	m
8.07.74	limestone	10.00	9.84	-0.168	4.70	2.50	0.020	0.20	-0.106	4.6
14.08.74	argillite	7.60	2.72	0.139	2.80	2.40	0.100	0.10	0.047	5.4
29.08.74	argillite,sandstone	7.60	2.96	0.151	3.60	2.55	0.020	0.06	-0.071	5.0
2.10.74	limestone	1.70	0.84							4.6
7.12.74	argillite	1.70	0.63							4.7
25.04.75	salt	0.35	8.27	0.156						
12.08.75	sandstone,aleurolite	7.60	2.54	0.129	2.60	2.40	0.125	0.06	0.006	5.2
29.09.75	salt	7.60	4.24	0.201	4.05	2.20			-0.082	4.8
29.03.76	salt	10.00	4.60	0.212						5.0
29.07.76	salt	58.00	2.58	0.132	4.60	2.20			-0.038	5.9
5.11.76	dolomite	15.00	6.18	-0.103	5.00	2.60		0.20	-0.024	5.3
26.07.77	salt	13.00	3.61	0.178	4.20	2.20			-0.074	5.0
10.08.77	granit	8.50	2.45	0.124	4.80	2.60			0.044	5.0
20.08.77	tuff	8.50	2.94	0.150	3.80	2.70		0.06	-0.149	5.0
10.09.77	argillite	7.00	2.88	0.147	3.80	2.70		0.10	-0.065	4.8
30.09.77	salt	9.30	7.13	0.177	4.60	2.20			0.032	5.0
14.10.77	salt	0.10	12.53	0.099						
30.10.77	salt	0.01	27.01	-0.081						
9.08.78	sandstone,aleurolite	22.00	2.03	0.098	3.90	2.10	0.050	0.07	0.062	5.6

Table 2

Date	Media	Yield	Hreduced	Mcor	Velocity	Density	Moisture	Gaseous	Dm	m
24.08.78	dolomite	19.00	2.16	-0.193	5.10	2.45	0.020	0.25	0.013	5.1
12.09.78	salt	0.08	13.55	0.088						
21.09.78	sandstone,aleurolite	16.00	3.52	0.175	3.50	1.95	0.060	0.07	0.085	5.2
7.10.78	dolomite	13.00	6.51	-0.110	5.00	2.60		0.20	-0.035	5.2
17.10.78	salt	73.00	2.32	0.117	4.60	2.20			-0.060	5.8
17.10.78	aleurolite,sandstone	23.00	2.11	0.104	2.20	2.15	0.090	0.09	-0.380	5.5
30.11.78	salt	0.06	15.07	0.073						
18.12.78	salt	103.00	1.34	0.041	4.60	2.20			-0.180	5.9
10.01.79	salt	0.50	7.32	0.173						
17.01.79	salt	65.00	2.48	0.126	4.60	2.20			-0.048	6.0
14.07.79	salt	21.00	3.56	0.176	4.60	2.20			0.030	5.6
12.08.79	dolomite	7.60	5.26	-0.081	4.50	2.40		0.20	-0.136	4.9
6.09.79	conglomerate tuff	7.60	3.21	0.162	3.50	2.50		0.08	-0.183	4.9
16.09.79	sandstone	0.30	13.50	0.088						
4.10.79	clay	21.00	3.03	0.154	2.15	1.70	0.150	0.10	-0.054	5.4
7.10.79	dolomite	15.00	6.28	-0.105	5.00	2.60		0.20	-0.027	5.0
24.10.79	salt	33.00	3.06	0.155	4.60	2.20			-0.002	5.8
16.06.80	limestone	3.00	9.70	-0.166						
25.06.80	limestone	3.00	9.01	-0.156						

Table 2

Date	Media	Yield	Hreduced	Mcor	Velocity	Density	Moisture	Gaseous	Dm	m
8.10.80	salt	8.50	5.15	0.222	4.05	2.20		0	-0.049	5.2
1.11.80	salt	8.00	3.62	0.178	4.12	2.30			-0.085	5.2
10.12.80	aleurolite,sandstone	15.00	10.10	0.129	4.30	2.60		0.00	-0.079	5.3
25.05.81	clay,aleurolite	37.60	4.51	0.209	2.40	2.46			-0.168	5.5
2.09.81	dolomite,limestone	3.20	14.18	-0.219	5.00	2.64		0.20	-0.201	4.4
26.09.81	salt	8.50	5.14	0.225	4.05	2.20			-0.049	5.2
26.09.81	salt	8.50	5.14	0.225	4.05	2.20			-0.049	5.3
22.10.81	dolomite	8.50	2.84	-0.155	4.90	2.70		0.20	-0.119	5.1
30.07.82	dolomite	8.50	4.18	-0.101						
4.09.82	sandstone	16.00	3.81	0.186	4.20	2.70			-0.008	5.3
25.09.82	gabbro,aleurolit	8.50	2.70	0.138						5.2
10.10.82	dolomite,argillite	16.00	5.99	-0.099	5.00	2.50		0.10	-0.322	5.3
16.10.82	salt	13.50	5.18	0.221	4.05	2.20			-0.050	5.4
16.10.82	salt	8.50	5.39	0.216	4.05	2.20			-0.058	5.2
16.10.82	salt	8.50	4.86	0.220	4.05	2.20			-0.052	5.2
16.10.82	salt	8.50	4.09	0.196	4.05	2.20			-0.089	5.2
10.07.83	salt,angidrite	13.50	3.85	0.187	4.40	2.20			-0.009	5.3
10.07.83	salt,angidrite	13.50	3.85	0.187	4.40	2.20			-0.009	5.3
10.07.83	salt,angidrite	13.50	3.53	0.175	4.40	2.20			-0.028	5.3

Table 2

Date	Media	Yield	Hreduced	Mcor	Velocity	Density	Moisture	Gaseous	Dm	m
24.09.83	salt	8.50	5.14	0.222	4.20	2.20			-0.006	5.2
24.09.83	salt	8.50	5.19	0.221	4.20	2.20			-0.070	5.1
24.09.83	salt	0.00	4.51	0.209	4.20	2.20			-0.026	5.0
24.09.83	salt	8.50	5.39	0.216	4.20	2.20			-0.015	5.2
24.09.83	salt	8.50	5.40	0.214	4.20	2.20			-0.018	5.4
24.09.83	salt	8.50	5.14	0.222	4.20	2.20			-0.006	5.3
21.07.84	salt	13.50	3.55	0.177	4.40	2.20			-0.021	5.4
21.07.84	salt	13.50	4.03	0.195	4.40	2.20			-0.023	5.3
21.07.84	salt	13.50	3.54	0.177	4.40	2.20			-0.021	5.4
11.08.84	clay,sandstone	9.50	3.58	0.178	2.60	2.10	0.100	0.09	-0.027	5.3
25.08.84	clay	8.50	3.56	0.177	1.80	2.00	0.200	0.10	-0.054	5.3
27.08.84	apatite ore	3.60	1.14	0.018	4.40	2.70	0.050		0.060	4.7
28.08.84	limestone	3.20	18.82	-0.258	4.10	2.64	0.080	0.20	-0.077	4.4
28.08.84	limestone	3.20	19.00	-0.259	4.10	2.64	0.080	0.20	-0.079	4.4
17.09.84	granit	10.00	2.59	0.132	4.00	2.70			-0.150	5.0
27.10.84	salt	3.20	6.79	0.184	4.20	2.20			-0.065	5.0
27.10.84	salt	3.20	6.79	0.184	4.20	2.20			-0.065	5.0
18.06.85	argillite,limestone	2.50	21.00	0.027	3.45	2.30		0.10	-0.409	
18.07.85	sandstone,aleurolite	8.50	3.78	0.185	4.00	2.30		0.05	-0.048	5.1

Table 2

Date	Media	Yield	Hreduced	Mcor	Velocity	Density	Moisture	Gaseous	Dm	m
19.04.87	limestone	3.20	13.95	-0.216	4.10	2.64	0.080	0.20	-0.012	4.5
19.04.87	limestone	3.20	13.67	-0.213	4.10	2.64	0.080	0.20	-0.003	4.5
7.07.87	dolomite,argillite	13.00	6.50	-0.110	5.00	2.50		0.10	-0.161	5.1
24.07.87	dolomite,argillite	13.00	6.44	-0.109	5.00	2.50		0.10	-0.159	5.1
12.08.87	salt	3.20	5.53	0.212	4.40	2.40			0.056	5.0
3.10.87	salt	8.50	4.90	0.221	4.12	2.30			-0.018	5.2
22.08.88	glay	16.00	3.29	0.166						5.3
6.09.88	angidrite	7.50	4.19	0.199						4.8

Table 3

Date	GMT,hhmmss	Distance	Baz	Ptime	Pmtime	T,sec	Amax
28.08.73	30000.035	341	206	46.33	50.85	0.64	0.315
18.06.85	40000.110	802	7	106.72	152.24	0.86	0.018
19.09.73	30000.180	839	193	108.50	110.41	0.42	4.280
4.10.79	160000.030	848	4	107.50	155.07	1.50	1.320
10.12.80	70000.060	978	350	125.71	178.02	0.64	0.130
25.08.84	190000.330	986	6	123.33	181.67	1.30	0.594
26.10.73	60000.000	989	279	127.05	130.55	0.81	0.122
15.08.73	20000.020	1145	192	149.28	150.13	0.58	0.097
10.07.83	40000.010	1168	268	150.52	153.30	0.62	0.400
10.07.83	40459.930	1167	268	150.60	153.82	0.68	0.406
10.07.83	40959.870	1165	268	150.33	153.71	0.64	0.286
21.07.84	25959.810	1167	268	150.24	153.85	0.56	0.437
21.07.84	30459.710	1164	268	150.47	153.49	0.60	0.269
21.07.84	30959.840	1166	268	150.48	153.23	0.62	0.435
17.10.78	140000.160	1200	343	152.29	164.02	1.04	0.243
2.09.81	35959.990	1214	319	145.33	150.21	0.28	0.015
11.08.84	190000.200	1583	333	199.92	211.59	0.68	0.170
30.09.77	65958.550	1662	258	207.85	211.40	0.62	0.095
29.07.76	50000.650	1666	258	207.56	213.70	0.72	0.640
14.07.79	50000.850	1668	258	204.92	208.70	0.50	0.349
24.10.79	55959.350	1667	258	208.00	211.43	0.54	0.429
18.12.78	75958.950	1665	258	207.65	212.63	0.94	0.854
21.09.78	150000.190	1711	24	215.90	226.92	0.63	0.760
8.10.80	60000.200	1711	255	213.41	216.66	0.84	0.136
26.09.81	50000.280	1710	255	213.13	216.20	0.80	0.139
26.09.81	50359.940	1713	255	213.28	215.95	0.78	0.137
16.10.82	60000.150	1717	255	213.40	216.48	1.00	0.137
16.10.82	60500.080	1716	255	213.72	216.40	0.82	0.133
16.10.82	61000.100	1717	255	213.64	216.05	0.88	0.105
24.09.83	50000.030	1710	255	213.99	217.19	0.84	0.131
24.09.83	50500.030	1711	255	213.17	215.93	0.80	0.102
24.09.83	51000.080	1711	255	213.02	215.97	0.96	0.068
24.09.83	51500.140	1713	255	213.12	216.08	0.68	0.112
24.09.83	51959.990	1714	255	213.77	216.27	0.90	0.119
24.09.83	52500.000	1714	255	213.32	216.27	0.88	0.113
27.10.84	60000.000	1714	255	214.10	217.98	0.80	0.066

Table 3

Date	GMT,hhmmss	Distance	Baz	Ptime	Pmtime	T,sec	Amax
27.10.84	60500.000	1714	255	213.70	215.80	0.82	0.045
1.11.80	130000.420	1845	52	231.85	236.92	0.70	0.251
4.09.82	180000.580	1887	14	234.40	244.03	0.60	0.253
11.04.72	60002.000	1856	203	230.41	239.17	1.04	0.098
25.05.81	50000.320	1901	339	236.79	242.79	0.90	0.247
29.09.75	110000.430	2066	22	259.72	263.02	0.80	0.174
20.08.77	220000.780	2016	42	255.80	261.44	0.44	0.035
26.07.77	170000.220	2102	22	258.62	263.12	0.79	0.258
10.09.77	160000.180	2300	64	283.46	284.53	0.60	0.260
9.07.72	70002.000	2419	276	291.96	293.02	0.76	0.032
7.10.78	235959.650	2667	52	316.61	318.79	1.00	0.081
7.10.79	210000.220	2681	52	316.49	318.41	1.00	0.052
10.10.82	50000.220	2667	52	315.08	318.41	0.64	0.067
24.08.78	180000.350	2703	42	317.73	326.53	0.71	0.106
12.08.79	180000.210	3157	51	357.02	381.24	0.94	0.031
9.08.78	180000.790	3295	47	367.27	394.73	0.97	0.088

Table 4.

date	dist,km	baz, deg	depth, m	yield,kt	media	Dt, sec
4/10/79	848	4	837	21	clay	47.5
19/09/73	839	193	615	6.3	aleurolite	1.9
25/08/84	986	6	726	8.5	clay	58.7
26/10/73	989	279	2026	10	limestone	3.5
21/09/78	1711	24	886	16	sandstone	11.8
08/10/80	1711	255	1050	8.5	salt	3.2

Table 5.

# phase	1	2	3
backazimuth	255.4	253.9	249.5
incident angle	37.3	44.5	41.3
relation λ_1/λ_2	0.009	0.007	0.031

Table 6.

# phase	1	2	3
backazimuth	274.1	270.0	251.0
incident angle	49.7	44.2	40.0
relation λ_1/λ_2	0.004	0.011	0.038

Figure captures

Figure 1. Map of peaceful nuclear explosions in the USSR. Events shown square with size scaled by magnitule. The Borovoye station marked by asterisk.

Figure 2. Plot-record section of vertical component displacement for some explosions in the distance range from 1600 to 2000 km. The time reduced to the first arrival of each explosions. A row marks the seismic phases.

Figure 3. The main profile of deep seismic sounding in the North Kazakhstan. The lines show the different parts of profile and the close circles show shot-points, and triangle is Borovoye station. P1, P2 are presumed head wave and reflected wave generated on the discontinuity in upper mantle at the depth about 150-200 km.

Figure 4. The typical amplitude-frequency responce of digital channels at Borovoye station, based on KS, KSM, DS, and DSM seismometers.

Figure 5. The example of record and explosion carried out in salt at the distance about 1700 km . The rows show the arrival of different phases.

Figure 6. The comparision of seismograms observed from explosions carried out to the North from Borovoye station with seismogram from explosions from another direction: distance about 850 km (a), distance about 990 km (b), and distance about 1720 km (c).

Figure 7. The examples of the polarization characteristics of P-waves from explosions in salt at the distance of 1160 km (a), and of 1715 km (b): trace 1 is recording of vertical component of motion, trace 2 is the biggest eigenvalue λ_1, trace 3 is the relation of eigenvalue λ_1/λ_2, trace 4 is backazimuth, and trace 5 is incident angle.

Figure 8. The dependence of magnitude, m from yield of explosion, q without madnitude correction (a) and with magnitude correction (b). The points are experimental data from Table 1.

Figure 9. Amplitude spectra of displacement of initial 2 sec of P-wave of four explosions in salt with yield: 103 kt (a), 58 kt (b), 23 kt (c), and 9.3 kt (d). Theoretical spectrum for yield 100 kt according to Evernden et all is presented by the line (e). Dates of explosions placed in the right corner of picture.

Figure 10. Amplitude spectra of displacement for the window from 3 to 5 sec relatively the first arrival time . Denotes are the same as at Figure 9.

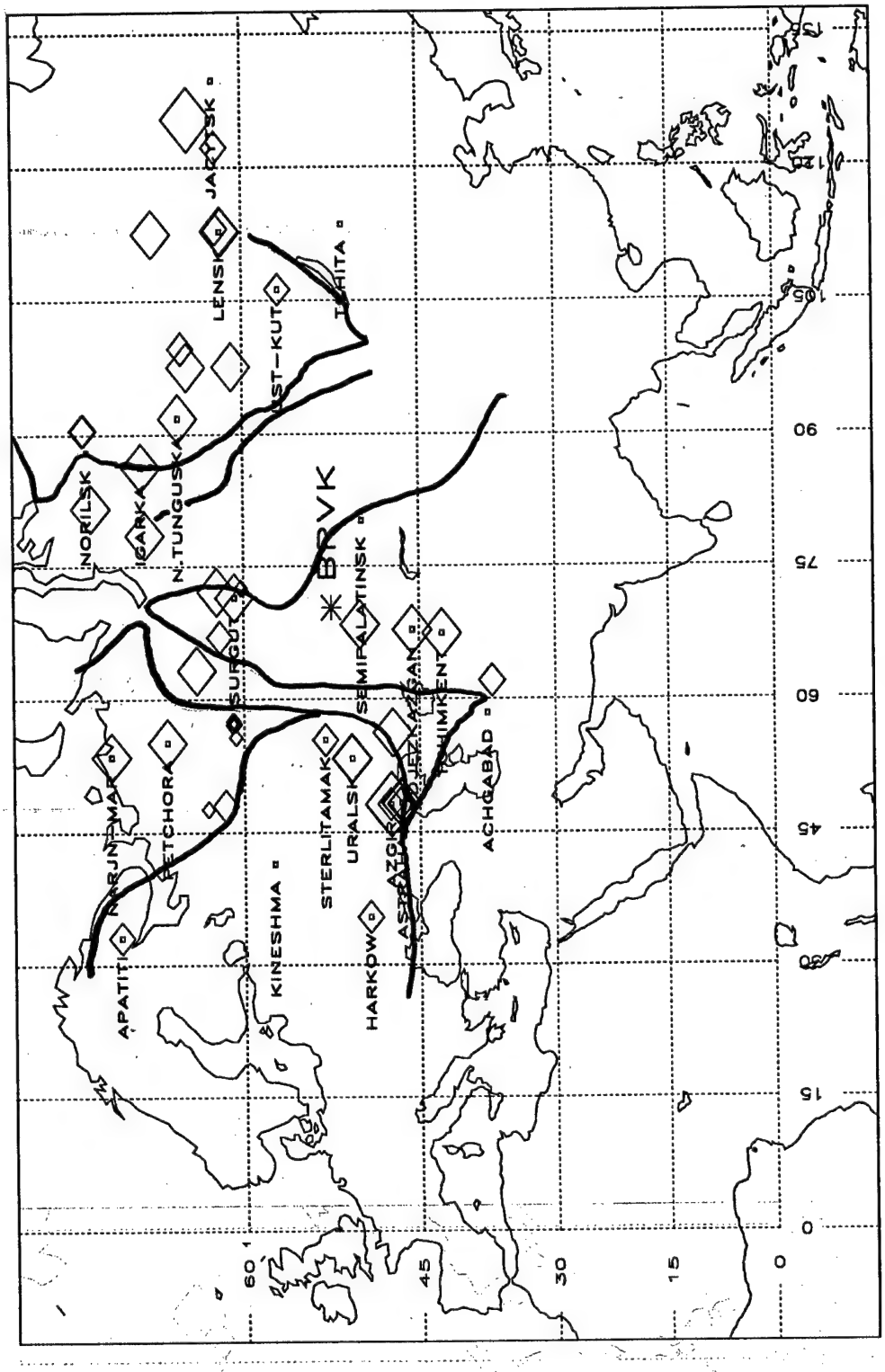
JAKUTSK
LENSK
TCHITA
UST-KUT
NORILSK
IGARKA
N.TUNGUSKA
SURGUT
BRVK
SEMIPALATINSK
STERLITAMAK
URALSK
TASHKENT
ACHGABAD
APATITY
KINESHMA
HARKOW
90
75
60
45
30
15
0
60

Figure 1

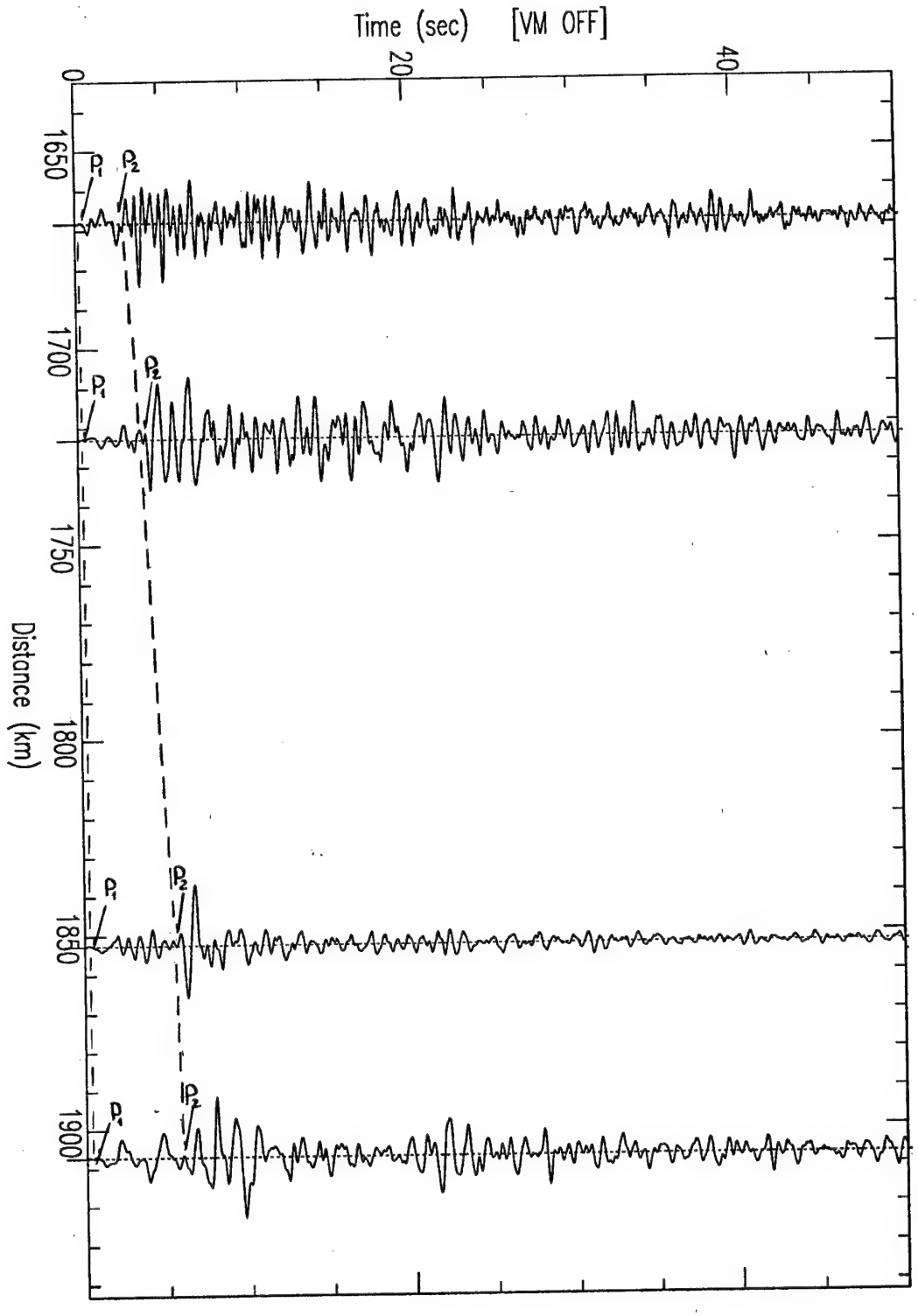
Time (sec) [VM OFF]
0
20
40
1650
1700
1750
1800
1850
1900
Distance (km)
P1
P2

Figure 2

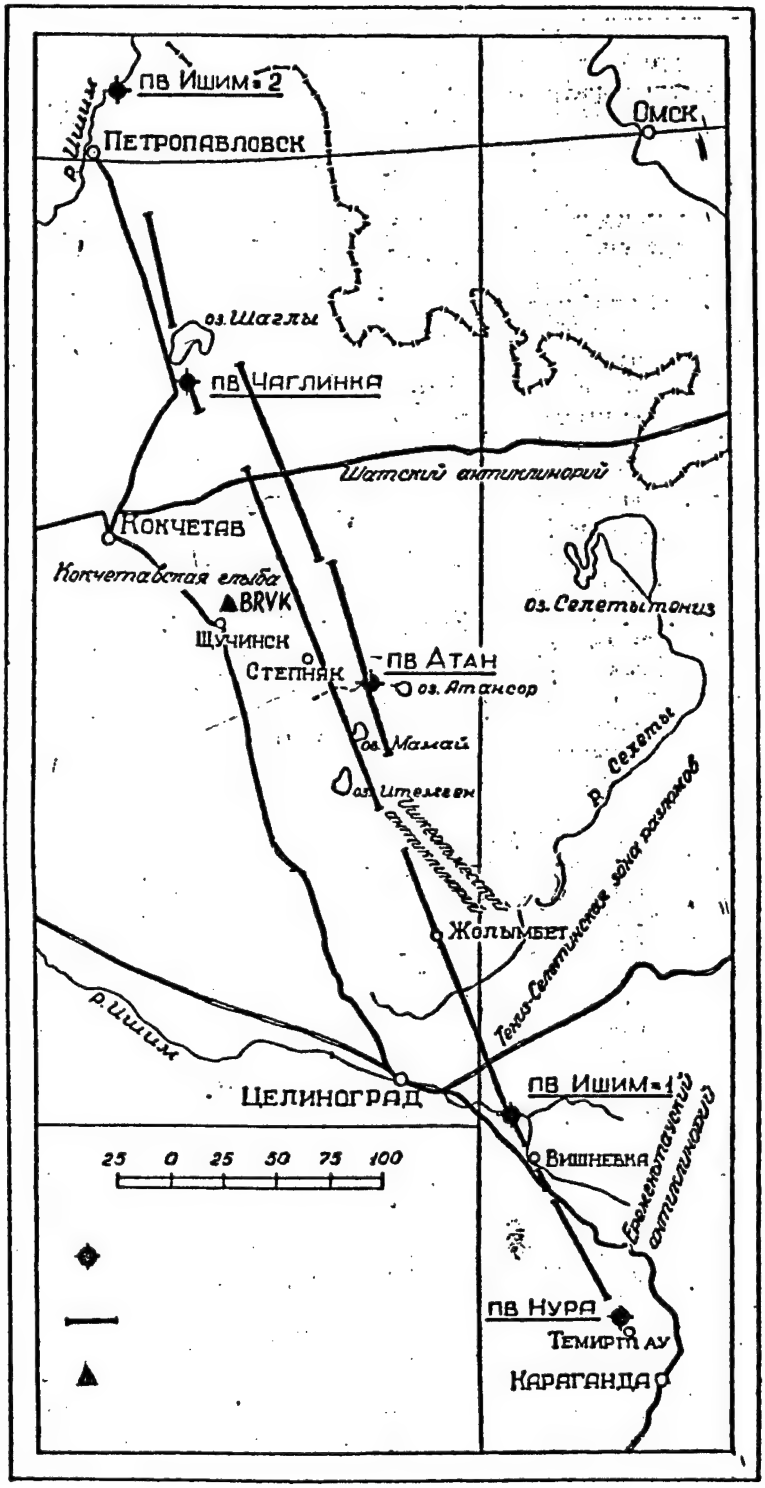
пв Ишим-2
р. Ишим
Петропавловск
Омск
оз. Шаглы
пв Чаглинка
Шатский антиклинорий
Кокчетав
Кокчетавская глыба
BRVK
Щучинск
Степняк
пв Атан
оз. Атансор
оз. Мамай
оз. Ителгван
Ишимский антиклинорий
оз. Селеты-тониз
р. Селеты
Жолымбет
Тенгиз-Селетинская зона разломов
р. Ишим
Целиноград
пв Ишим-1
Вишневка
Ерементауский антиклинорий
пв Нура
Темиртау
Караганда
25 0 25 50 75 100

Figure 3

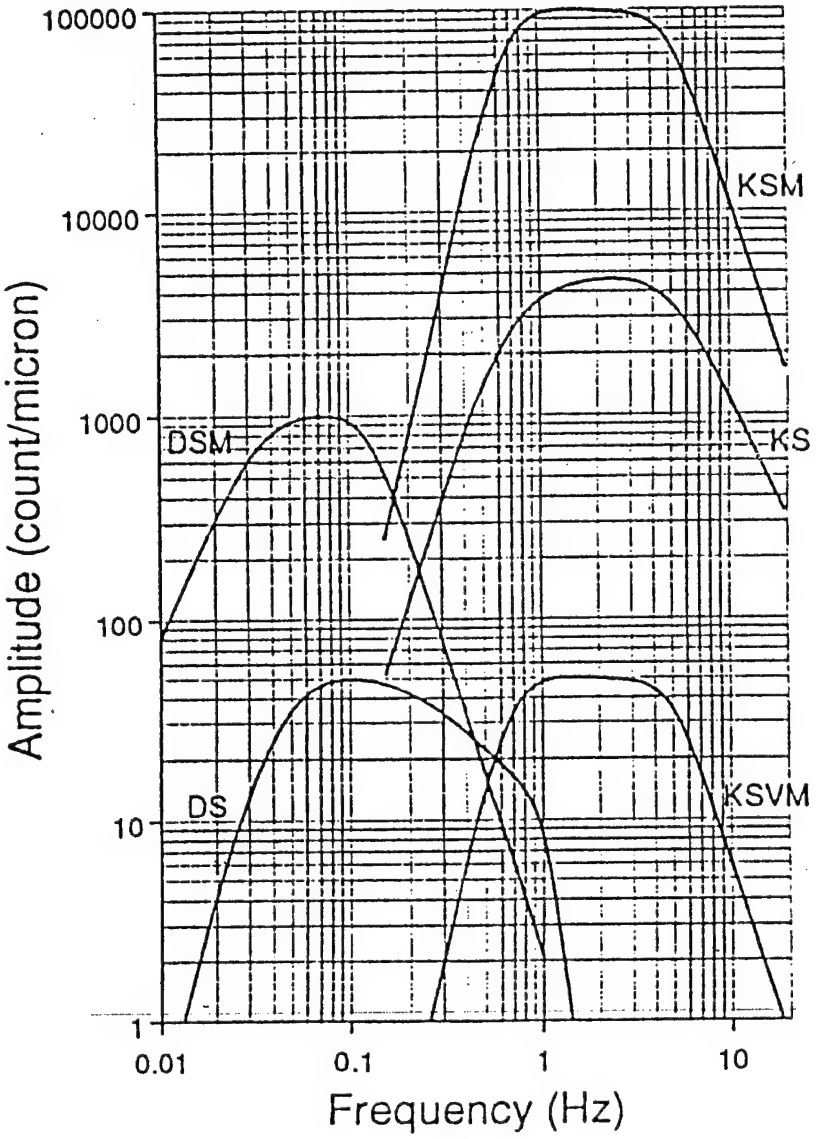
100000
10000
1000
100
10
1
Amplitude (count/micron)
KSM
KS
KSVM
DSM
DS
0.01
0.1
1
10
Frequency (Hz)

Figure 4

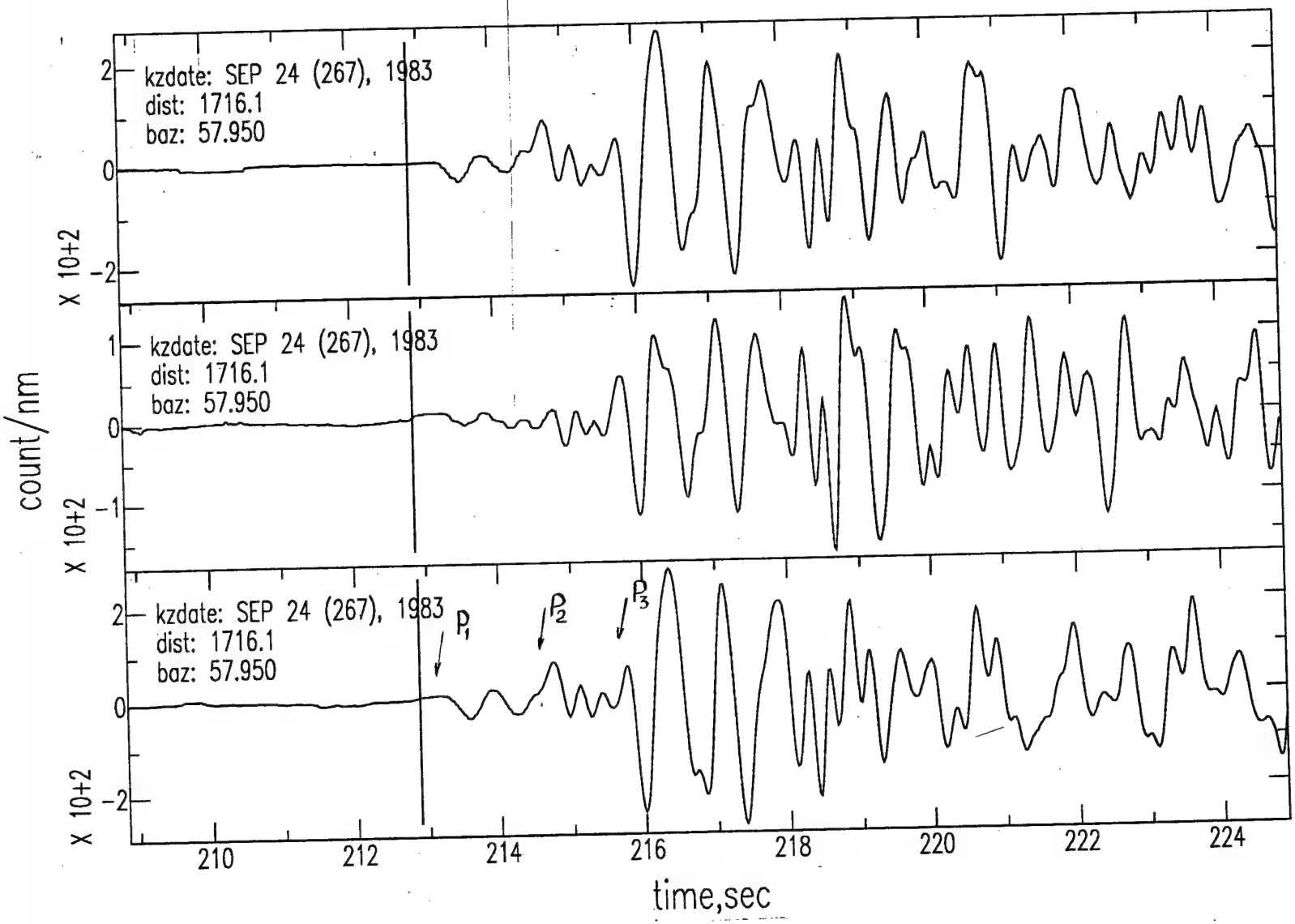
kzdate: SEP 24 (267), 1983
dist: 1716.1
baz: 57.950
X 10+2
kzdate: SEP 24 (267), 1983
dist: 1716.1
baz: 57.950
X 10+2
kzdate: SEP 24 (267), 1983
dist: 1716.1
baz: 57.950
P1
P2
P3
X 10+2
count/nm
time,sec

Figure 5

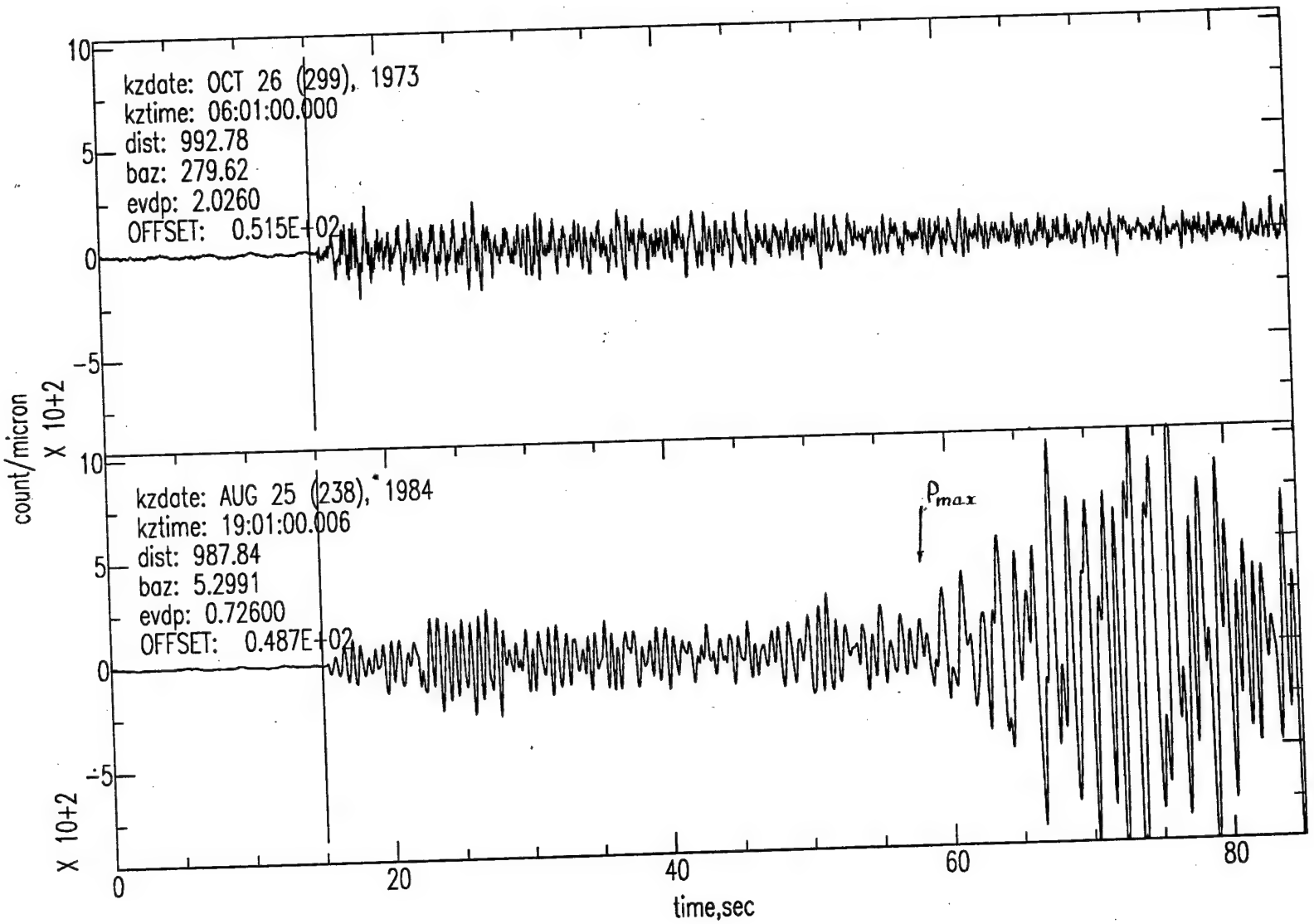
kzdate: OCT 26 (299), 1973
kztime: 06:01:00.000
dist: 992.78
baz: 279.62
evdp: 2.0260
OFFSET: 0.515E+02
kzdate: AUG 25 (238), 1984
kztime: 19:01:00.006
dist: 987.84
baz: 5.2991
evdp: 0.72600
OFFSET: 0.487E+02
P_{max}
count/micron
X 10+2
X 10+2
time,sec
10
5
0
-5
10
5
0
-5
0
20
40
60
80

Figure 6 a)

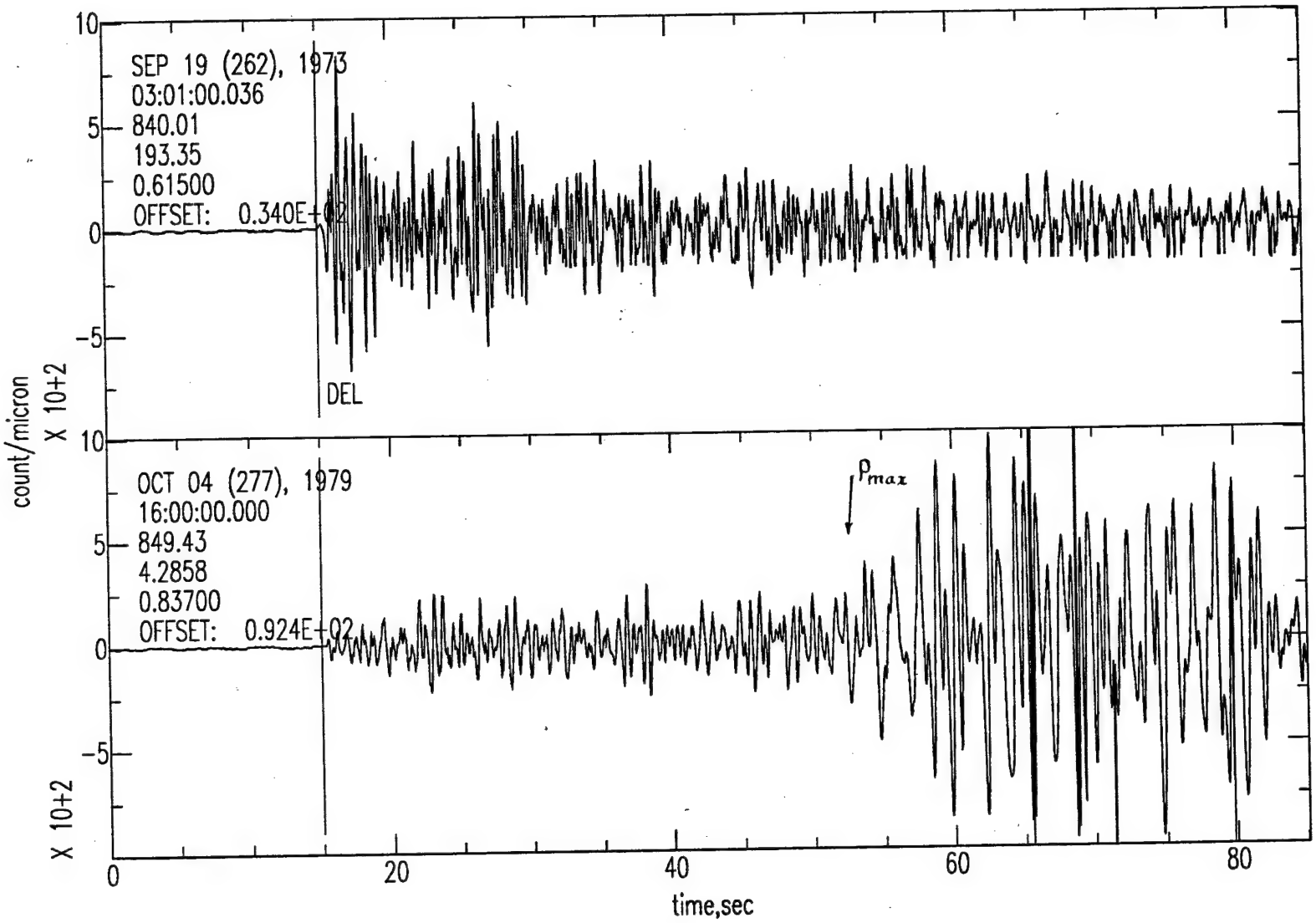
SEP 19 (262), 1973
03:01:00.036
840.01
193.35
0.61500
OFFSET: 0.340E+02
DEL
OCT 04 (277), 1979
16:00:00.000
849.43
4.2858
0.83700
OFFSET: 0.924E+02
ρ_{max}
count/micron
X 10+2
X 10+2
time,sec
10
5
0
-5
20
40
60
80

Figure 6 b)

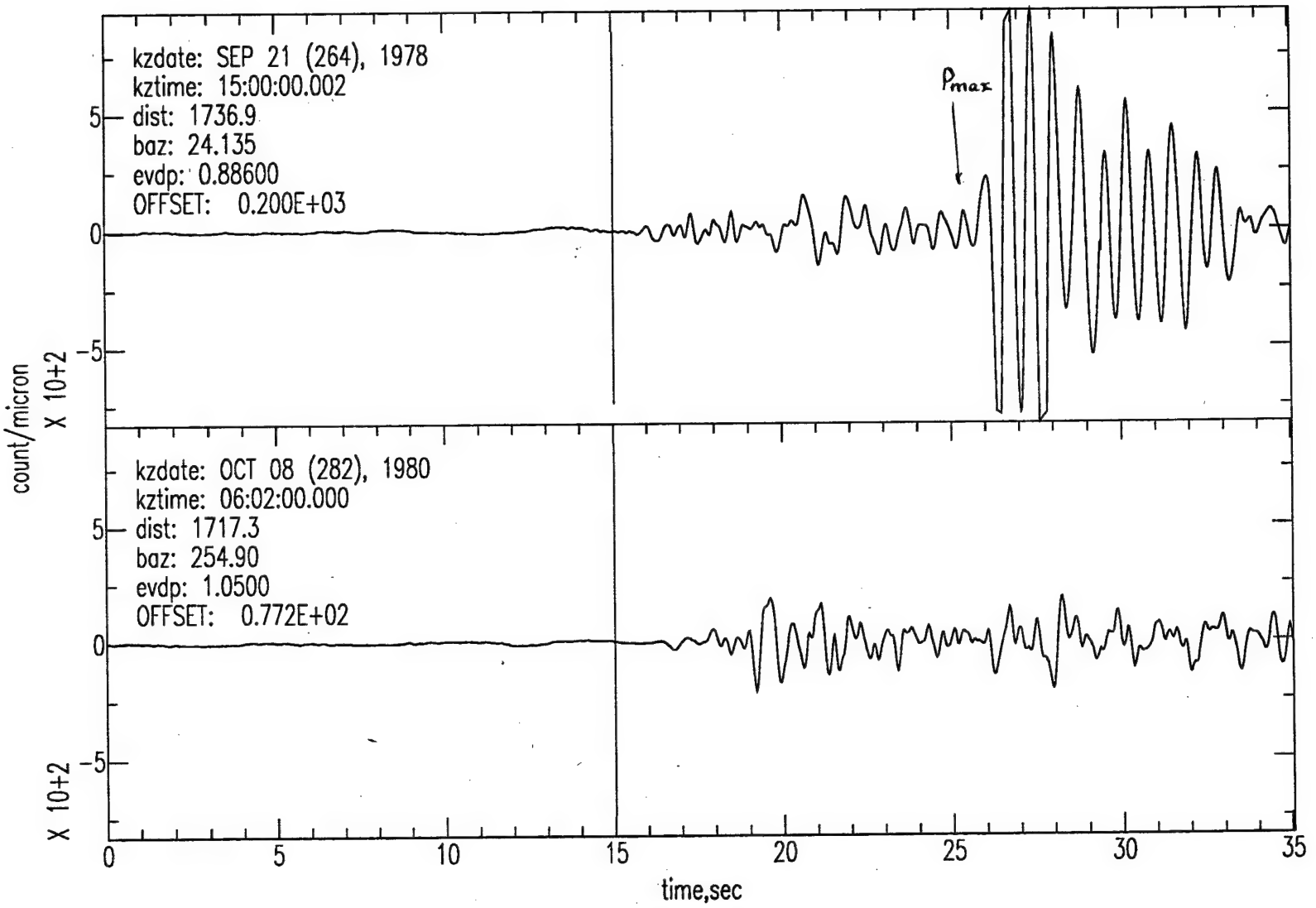
kzdate: SEP 21 (264), 1978
kztime: 15:00:00.002
dist: 1736.9
baz: 24.135
evdp: 0.88600
OFFSET: 0.200E+03
P max
kzdate: OCT 08 (282), 1980
kztime: 06:02:00.000
dist: 1717.3
baz: 254.90
evdp: 1.0500
OFFSET: 0.772E+02
count/micron
X 10+2
X 10+2
5
0
-5
5
0
-5
0
5
10
15
20
25
30
35
time,sec

Figure 6 c)

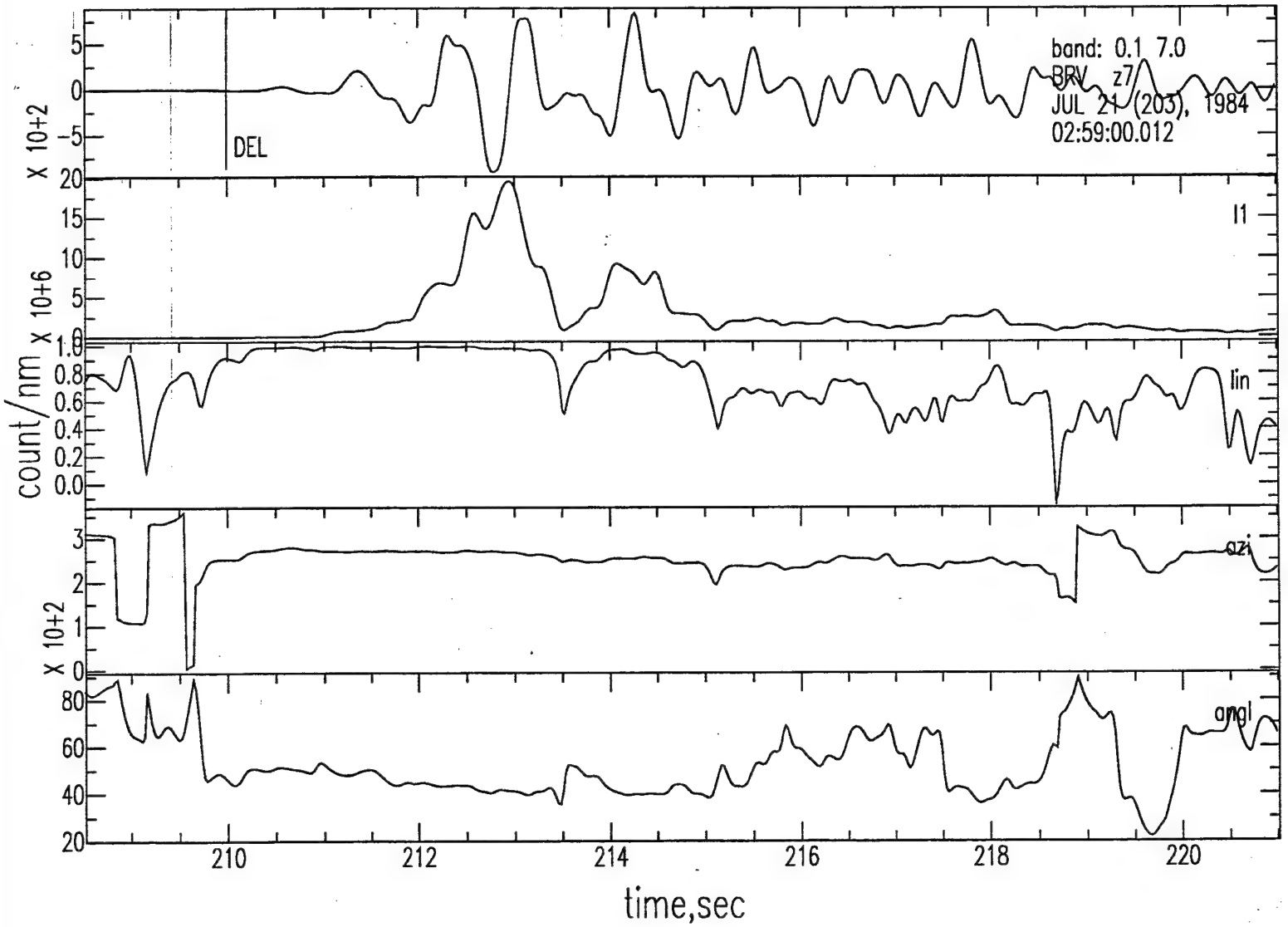
band: 0.1 7.0
BRV z7
JUL 21 (203), 1984
02:59:00.012
DEL
X 10+2
I1
X 10+6
lin
count/nm
azi
X 10+2
angl
time,sec

Figure 7 a)

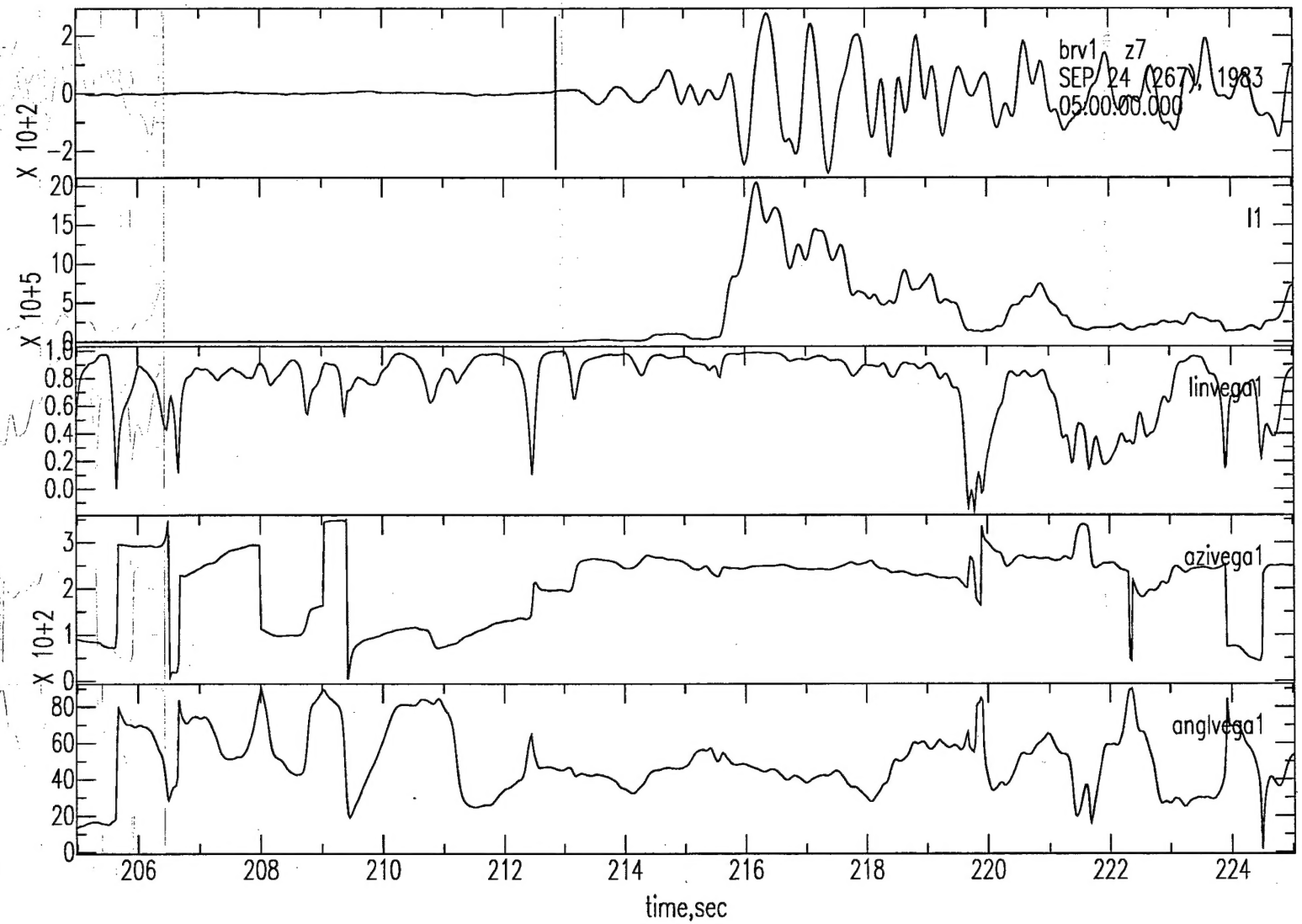
brv1 z7
SEP 24 (267), 1983
05:00:00.000
X 10+2
I1
X 10+5
linvega1
azivega1
X 10+2
anglvega1
time,sec

Figure 7 b

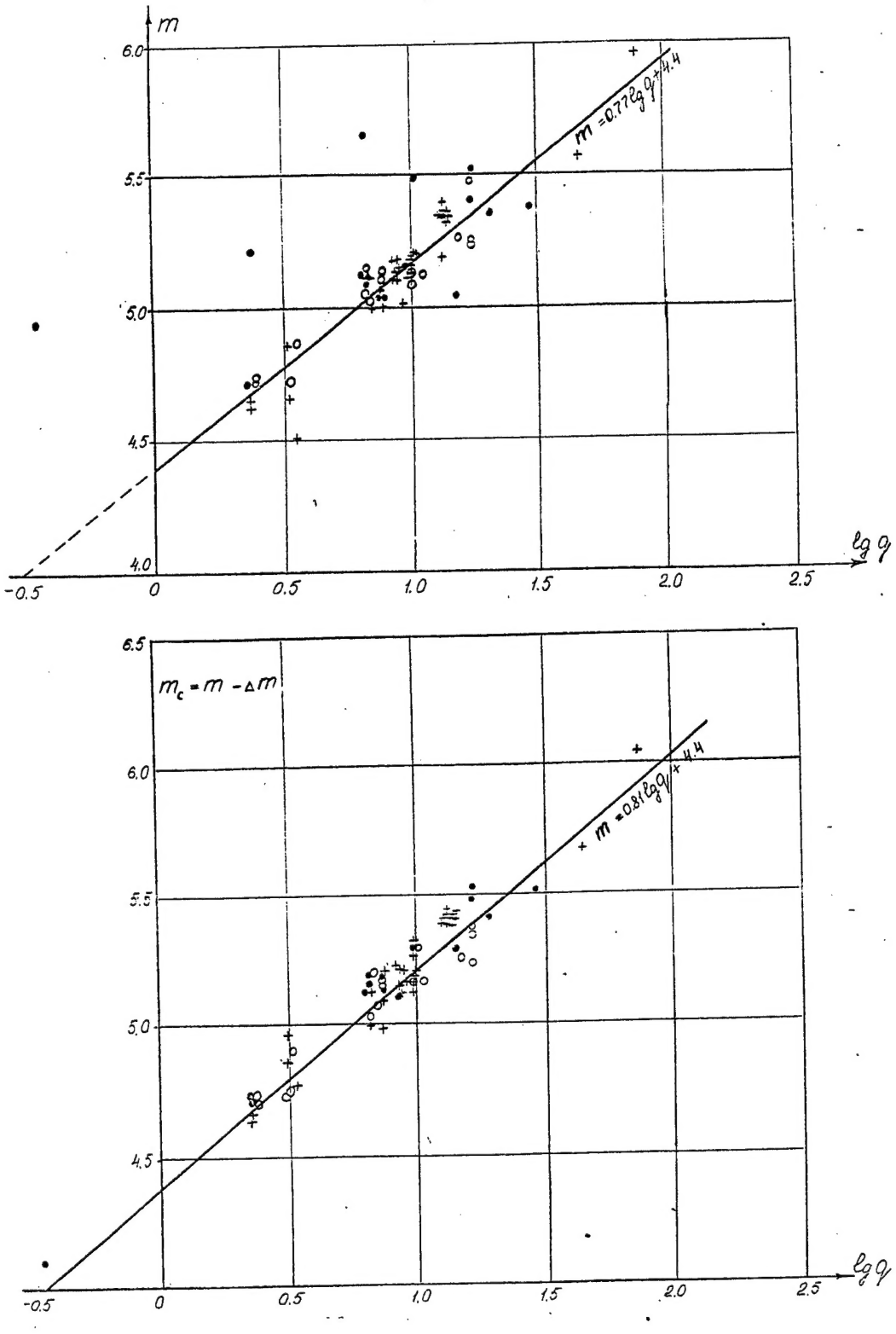
m
6.0
5.5
5.0
4.5
4.0
-0.5
0
0.5
1.0
1.5
2.0
2.5
lg q
m = 0.77 lg q + 4.4
$m_c = m - \Delta m$
6.5
6.0
5.5
5.0
4.5
m = 0.81 lg q + 4.4

Figure 8

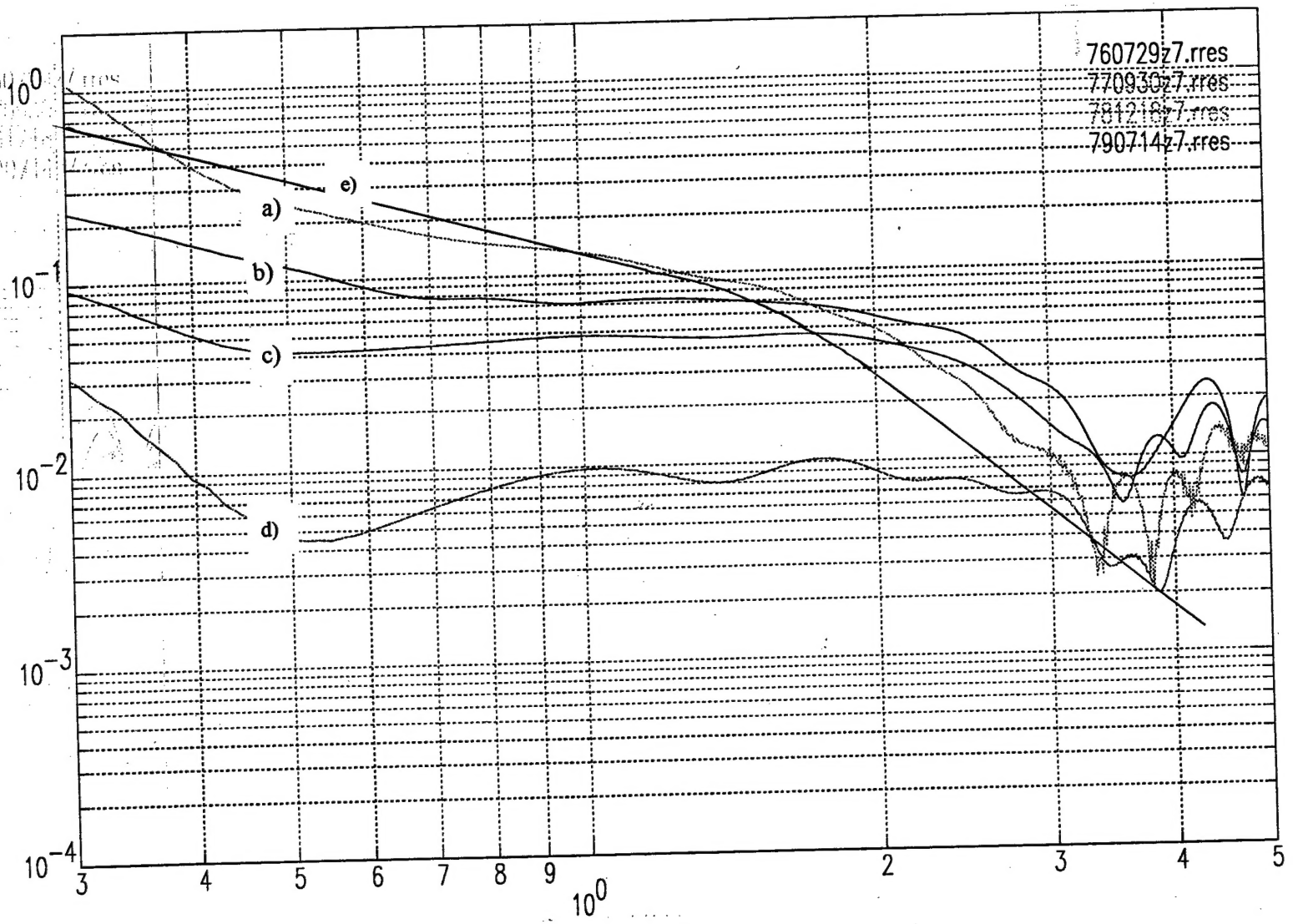
760729z7.rres
770930z7.rres
781218z7.rres
790714z7.rres
a)
b)
c)
d)
e)
10^0
10^{-1}
10^{-2}
10^{-3}
10^{-4}
3
4
5
6
7
8
9
10^0
2
3
4
5
Frequency, Hz

Figure 9

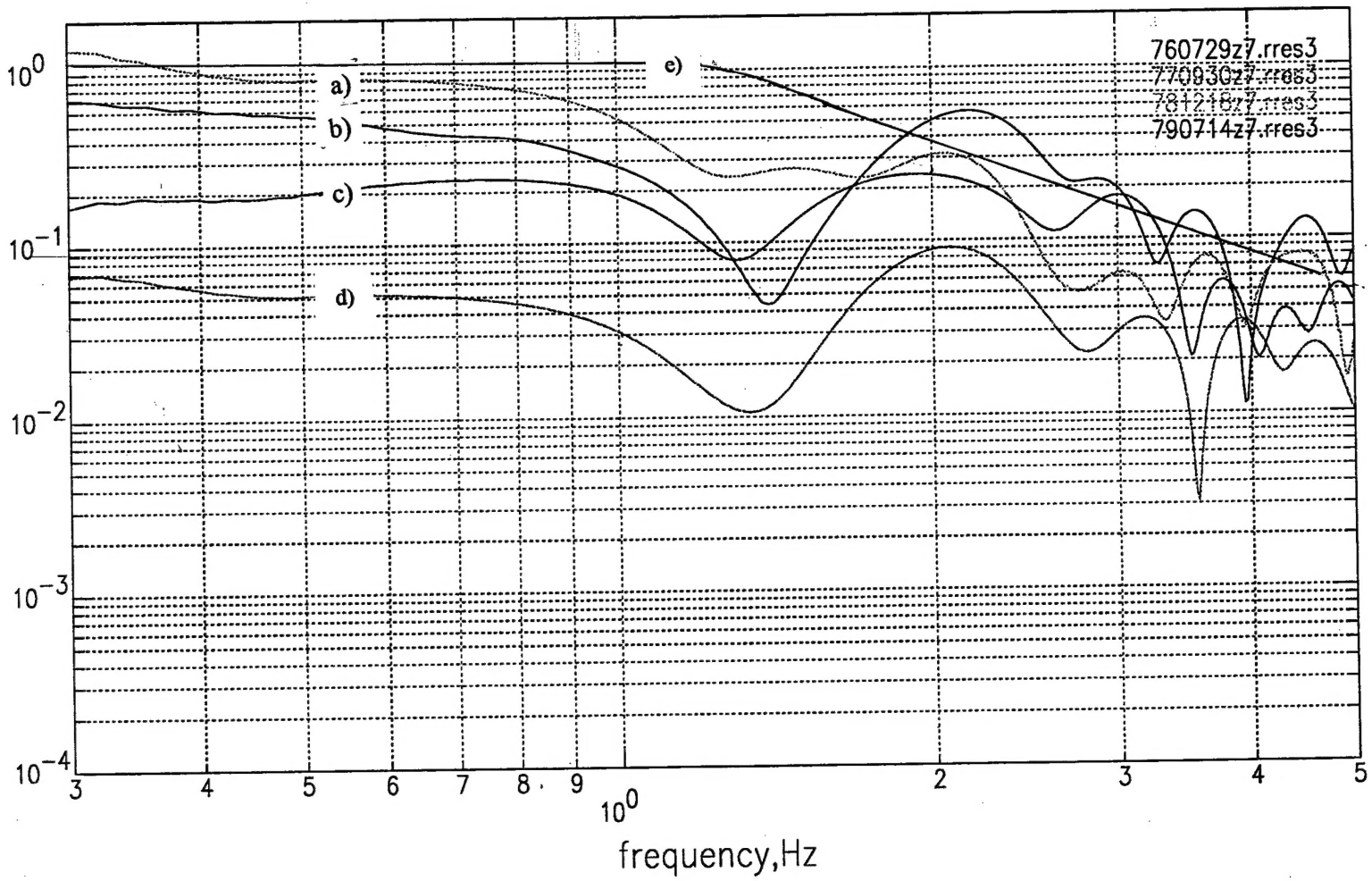
760729z7.rres3
770930z7.rres3
781218z7.rres3
790714z7.rres3
a)
b)
c)
d)
e)
10^0
10^{-1}
10^{-2}
10^{-3}
10^{-4}
3
4
5
6
7
8
9
10^0
2
3
4
5
frequency,Hz

Figure 10